Paper III

Depositional facies and reservoir quality of deep-marine sandstones in the Norwegian Sea

Trond Lien, Ruth Elin Midtbø & Ole J. Martinsen

Lien, T. Midtbø, R.E. & Martinsen, O.J.: Depositional facies and reservoir quality of deep-marine sandstones in the Norwegian Sea. *Norwegian Journal of Geology*, Vol. 86, pp. 71-92. Trondheim 2006. ISSN-029-196X.

During the Late Cretaceous and Early Paleocene, deep-water depositional systems deposited sandstones in the Norwegian Sea. The reservoir quality is variable and difficult to predict because of variations in facies, burial depth and temperature history. High- and low-density turbidity currents were the dominant transportation processes of these sands, but debris flow deposits and cross-laminated sediments deposited by sustained sea floor currents occur. The grain size and total clay content have a major influence on the reservoir quality. Reservoirs deposited by turbidity currents have the coarsest and most clay-poor sediments, and the highest porosity and permeability.
Superimposed on the facies related reservoir quality trends, is a general trend of decreasing porosity and permeability with increasing burial depth. Given similar facies and similar burial depth, variation in the temperature and burial history results in completely different reservoir qualities. High heat flow and late structural uplift resulted in anomalously poor reservoir quality at present burial depth.

Norsk Hydro Research Center, Box 7120, NO-5020 Bergen, Norway (E-mail: Trond.Lien@hydro.com)

Introduction

Deep-marine sediments in the Norwegian Sea have during the last decade become increasingly important in exploration, and recently also in reservoir production. Several exploration wells have been drilled during the last few years discovering thick intervals of sand-rich deep-marine sediments of Late Cretaceous and Paleocene age. The reservoir quality of the sandstones is variable and difficult to predict because of the variation in facies, a generally deeply buried setting and variable temperature history.

This paper describes the sedimentary facies of the deep-marine deposits in the Norwegian Sea, and discusses the link between depositional facies and the variation in porosity and permeability of the sandstones. Further, other factors controlling the variation in porosity and permeability of these deep-marine sandstones are discussed. Factors that cause anomalously high porosity and permeability are discussed widely in the literature, however, many of these studies focus on deeply buried shallow-marine reservoirs with grain coats (e.g. Bloch et al. 2002). Our study focuses on quantification and predictability of porosity and permeability in deep-marine reservoirs. The aim is to illustrate how factors such as the depositional processes, sediment source area and burial and temperature history control the reservoir quality of deep-marine deposits in the Norwegian Sea.

Study area and database

The study area covers the Norwegian Sea from the Agat area (quadrant 35) in the south to the Vestfjord basin (quadrant 6610) in the north, including both the Møre and Vøring basins in the west and the structural terraces and platform areas in the east (Fig. 1). The database (Table 1) includes sedimentologically described cored intervals from the Cretaceous and Paleocene (Fig. 2) in 26 wells. Core porosity and permeability measurements were available for all wells in the database. The measurements were performed on standard core plugs, normally taken every 25 cm of the cored intervals. Petrographical analytical methods used are modal analyses of thin sections and X-ray diffraction (XRD) of bulk samples. A total of 297 modal analyses and 345 XRD analyses were used in this study.

Only 4 of the 26 wells described contain hydrocarbon accumulations. These reservoirs are all at relatively shallow burial depths, and no preservation of porosity and permeability from hydrocarbon emplacement can be recognized. Therefore, and because of the controversial literature on the overall effect of hydrocarbon emplacement on reservoir quality (Bloch et al. 2002), this aspect is not discussed further in this study.

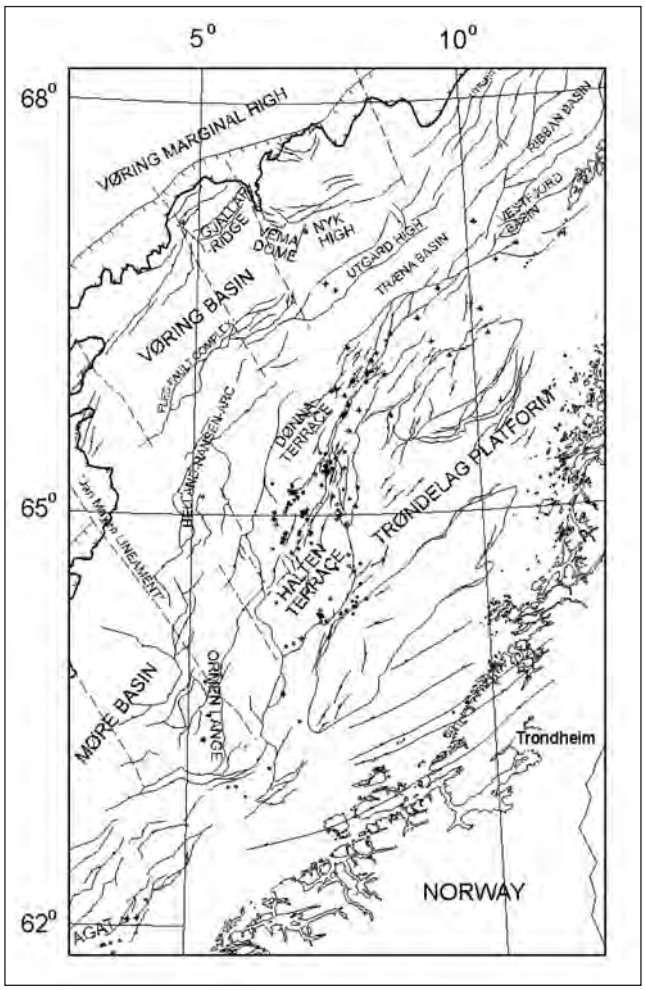

Fig. 1. Location map of the study area, Norwegian Sea.

Stratigraphy and tectonic development

The Cretaceous evolution in the Norwegian Sea is defined as a post-rift (thermal subsidence) period following Jurassic-earliest Cretaceous rifting and precedes a Late Cretaceous - Paleocene rift episode (Fig. 2; Færseth & Lien 2002). The extensional episode in the Late Cretaceous culminated with the opening of the northeast Atlantic Ocean in the Late Paleocene/Early Eocene (e.g. Skogseid & Eldholm 1989; Roberts et al. 1997). After the extensional episode, a Late Paleogene compressional phase initiated inversion of older Cretaceous subbasins such as the Ormen Lange Dome (e.g. Doré & Lundin 1996; Vågnes et al. 1998). Later, during the Pliocene and Pleistocene, the Norwegian mainland and easternmost parts of the Norwegian shelf experienced tectonic uplift probably caused by isostatic response to erosion by major glaciations (Riis 1996; Brekke 2000).

The Cretaceous and Paleocene stratigraphy is shown in Figure 2 and the stratigraphic nomenclature used is according to the formal stratigraphy for Mid-Norway (Dalland et al. 1988). The stratigraphy of the Early Cretaceous in the Norwegian Sea consists of the Lyr and Lange formations (Fig. 2). The sediments are dominated by deep-marine mudstones and thin sandstones deposited in basin lows, onlapping topographic highs, created by the Late Jurassic/Early Cretaceous rifting (Færseth & Lien 2002). The Late Cretaceous stratigraphy is divided into the Lysing, Kvitnos, Nise and Springar formations (Fig. 2). The Lysing Formation is dominated by deep-marine sandstones deposited on

Table 1.

Area	Wells	Formation	TS-data	XRD-data	Por. - Perm. data
Agat	4	Lysing	x	x	x
		Lange	x	x	x
Møre Margin	5	Lysing			x
		Lange			x
Møre Basin	3	Tang	x	x	x
		Springar	x	x	x
		Lysing		x	x
Halten Terrace	4	Lysing	x	x	x
		Lange	x	x	x
Dønna Terrace	4	Lysing	x	x	x
		Lange	x	x	x
Vestfjord Basin	1	Nise	x	x	x
		Kvitnos	x	x	x
		Lysing	x	x	x
Vøring Basin	5	Tang			x
		Springar	x	x	x
		Nise	x	x	x
		Kvitnos	x	x	x
		Lysing			x

Table 1. Database showing area, number of wells within each area, lithostratigraphic formation, available porosity measurements, number of thin-sections and XRD (x-ray diffraction) measurements.

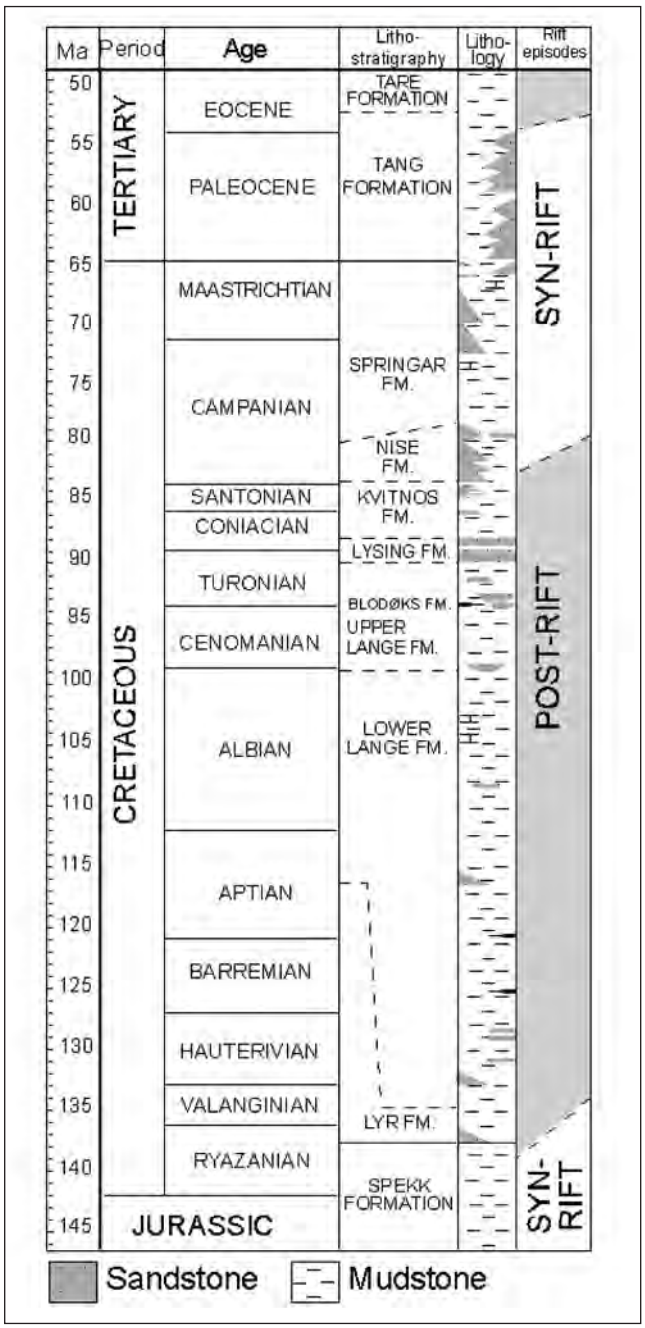

Fig. 2. Stratigraphy of the Cretaceous and Paleocene in the Norwegian Sea.

Table 2. Facies classification

Facies	Subfacies	Depositional process
A. Massive sandstones	A1. Amalgamated sandstones	High-density turbidity current
	A2. Interbedded massive sandstones	High-density turbidity current
	A3. Dewatered A1 (A1/3) and A2 (A2/3)	High-density turbidity current, modified by dewatering
B. Graded and laminated sandstones	B1. Interbedded graded sandstones	Low-density turbidity current
	B2. Interbedded laminated sandstones	Sustained strong seafloor currents
C. Heterolithic sediments and mudstones	C1. Heterolithic sediments	Low-density turbidity current, weak seafloor currents
D. Deformed sediments	D1. Injected sandstones	Post depositional deformation by loading and injection
	D2. Slides/Slumps	Post depositional deformation by sliding and slumping
E. Debris flows	E1. Debris flows	Plastic flows

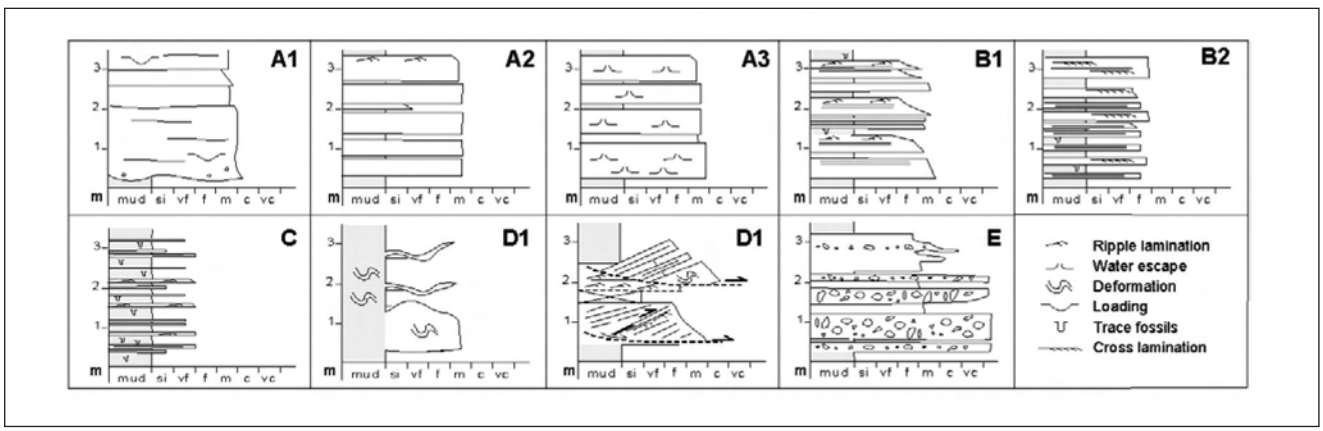

Fig. 3. Facies classification. Facies A1: Amalgamated massive sandstone, Facies A2: Interbedded massive sandstone, Facies A3: Massive sandstone with fluid escape structures, Facies B1: Interbedded graded sandstone, Facies B2: Interbedded laminated sandstone, Facies C: Heterolithic sediments, Facies D1: Injected sandstone, Facies D2: Slides/Slumps and Facies E: Debris flows. See also Table 2.

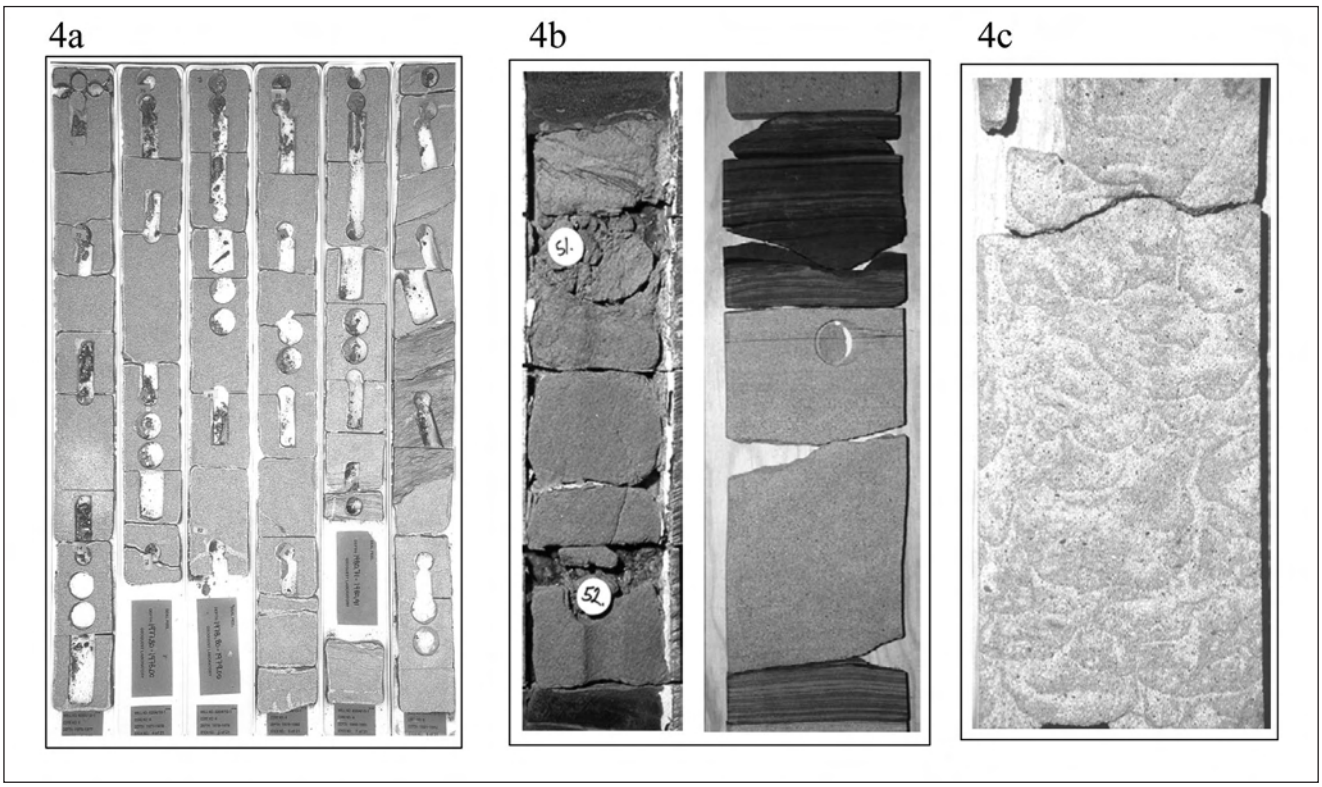

Fig. 4. Core photos of Facies A
a) Subfacies A1: Amalgamated massive sandstone, Lysing Formation, well 6204/10-1
b) Subfacies A2: Interbedded massive sandstone. Left: well 6707/11-1, Nise Formation. Note rippled top. Right: Well 35/3-5, Lange Formation.
c) Subfacies A3: Amalgamated massive sandstone deformed by fluid escape. Note the dish structures with edges curving up into sub-vertical fluid escape pipes, Agat, well 35/3-5. Core is 10 cm wide.

regional basin slopes like the Halten- and Dønna Terraces and the Agat area (Martinsen et al. 2005). The Kvitnos, Nise and Springar formations are dominated by deep marine mudstones, but thick, local sandstone intervals occur in the Vøring Basin. These sandstones were deposited in a deep-marine environment, where local basin topography and subsidence were influenced by the early stage of the Late Cretaceous/Paleocene rifting (Færseth & Lien 2002). Sandstone of Paleocene age (Tang Formation) is deposited in locally deep-marine sub-basins in the Møre Basin (Ormen Lange Dome) and Vestfjord Basin (Fig.1) developed during the Late Cretaceous/Early Paleocene syn-rift stage. In general, the Upper Cretaceous sandstones deposited in the Vøring Basin are sourced from East Greenland, while the Upper Cretaceous and Paleocene sandstones deposited in the Vestfjord Basin, eastern Møre Basin and Halten/Dønna Terrace are sourced from the mid-Norwegian margin. The sandstones deposited in the Agat area are, however, sourced from the western Norwegian mainland (Fonneland et al. 2004).

The Cretaceous and Paleocene form important reservoir intervals in the Møre and Vøring basins where sediments of up to 8 km in thickness were deposited (Færseth & Lien 2002). Major thickness variations of Cretaceous sediments occur due to pre-existing differences in topography following Jurassic crustal stretching as well as Cretaceous differential compaction across Jurassic normal faults (Færseth & Lien 2002).

The tectonic history, including differential subsidence during the Cretaceous post-rift phase and the latest Cretaceous/Early Paleocene rift episode, and Paleogene/Neogene compression and tectonic uplift, caused different temperature and burial histories between the different areas in the Norwegian Sea basins. This variability, together with variation in sediment source areas and depositional processes that varied in time and space, make prediction of reservoir quality in the present day deep-water reservoirs of the Norwegian Sea very challenging.

Facies of the deep-water sediments in the Norwegian Sea

The Cretaceous and Early Paleocene strata in the Norwegian Sea were deposited in a deep-water environ-

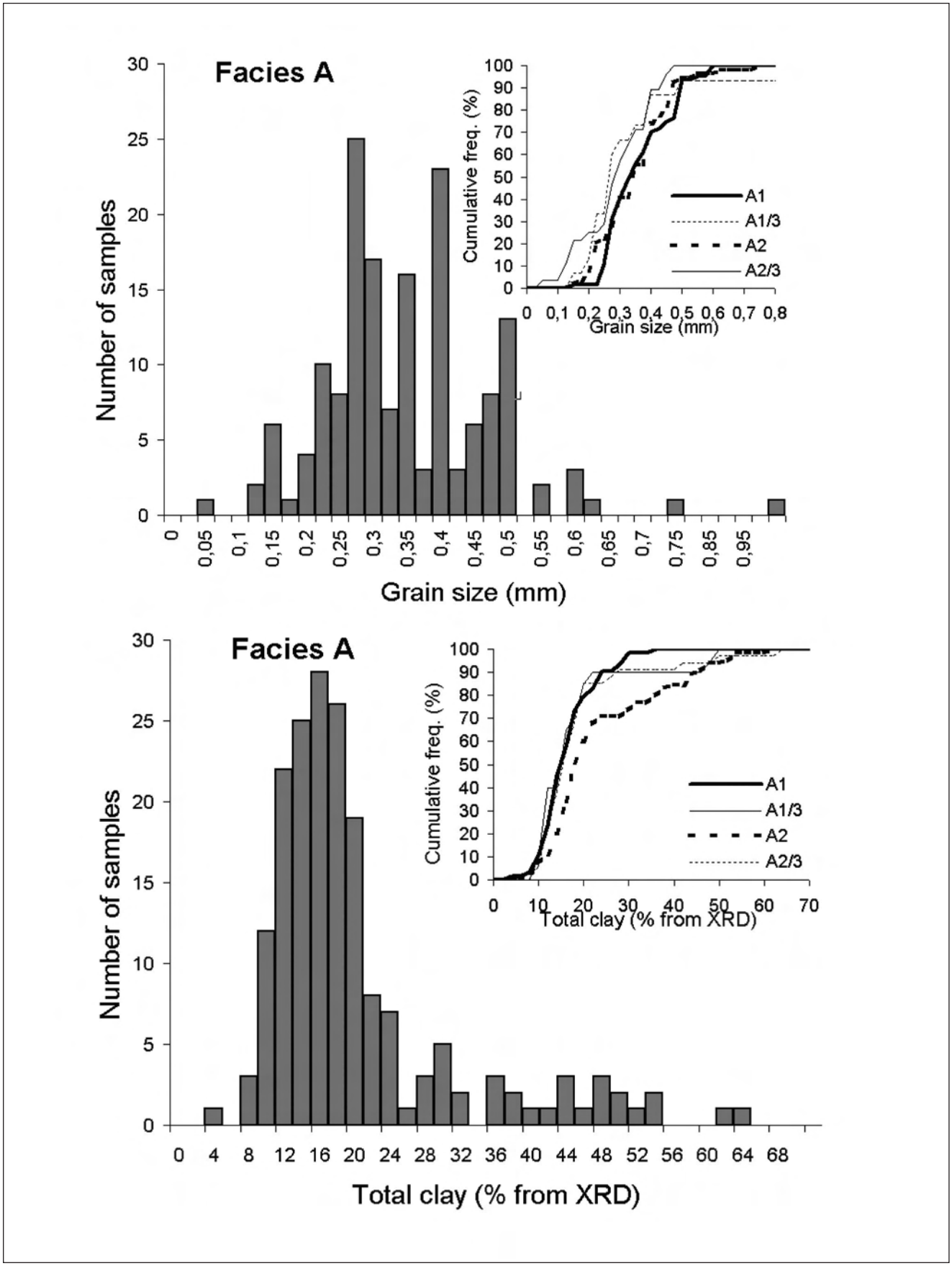

Fig. 5. Petrology of Facies A with grain size distribution and total clay content. Curves in upper right corners show the cumulative frequency of grain size and total clay content, separated by the subfacies A1, A2 and A3. Note: A1/3 is subfacies A1 deformed by fluid escape; A2/3 is subfacies A2 deformed by fluid escape.

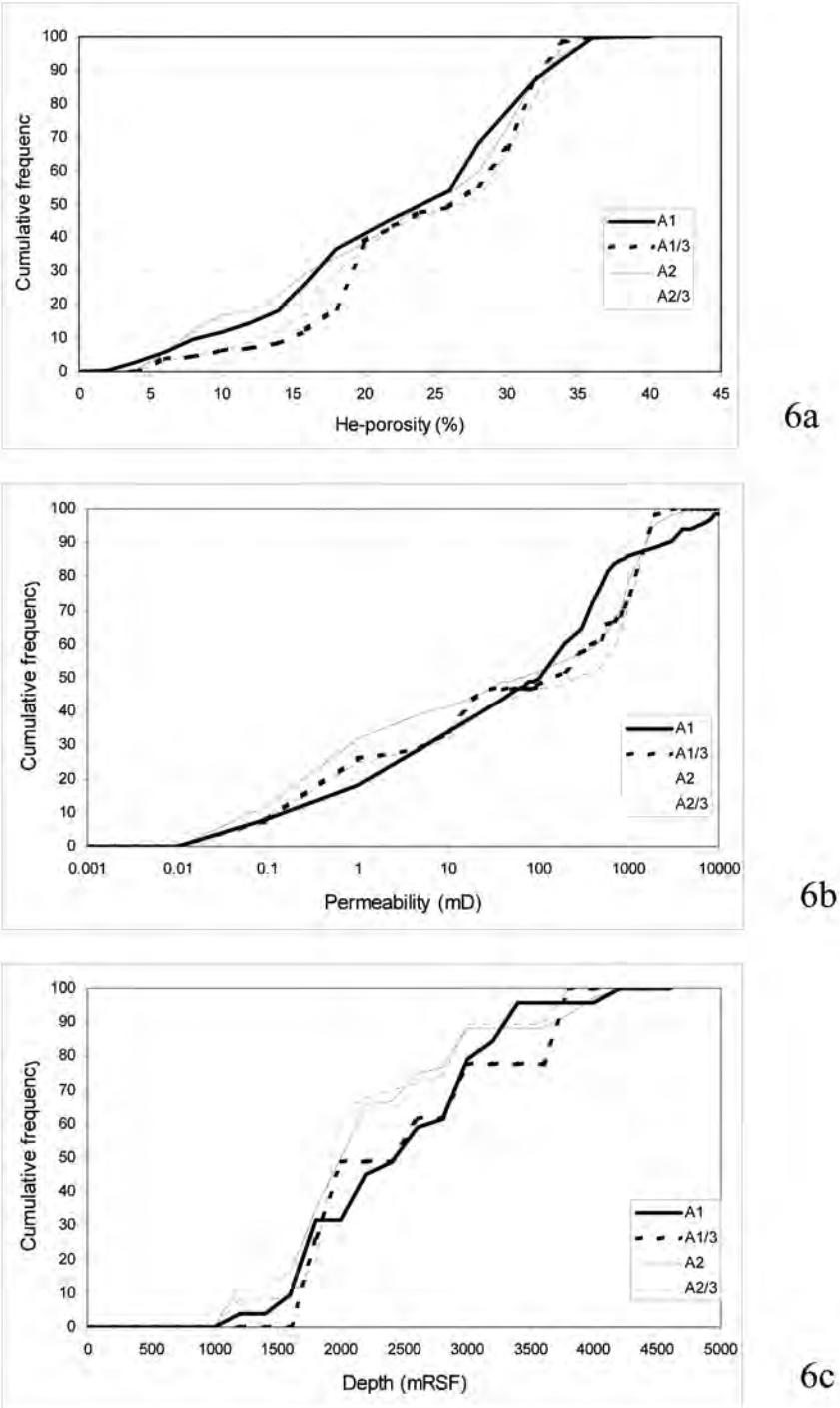

Fig. 6. Cumulative frequency of the Porosity and Permeability of Facies A
a) Porosity of Facies A
b) Permeability of Facies A
c) Burial depth of Facies A

ment, and are grouped into 5 main facies (facies A - E, Table 2 and Fig. 3). The facies division is based on lithology and interpreted depositional processes. The 5 main facies are further divided into subfacies (i.e. A1 and A2, Table 2). The subdivision is based on minor differences in depositional processes, and thereby lithology, within the main facies. The facies classification relies on our understanding of the terms *Bouma turbidites/divisions*, and *low- and high-density turbidites*, and is based on classical work on turbidite facies by Bouma (1962) and Lowe (1982).

In the following section, a description of the facies and interpretation of their depositional processes is presented. The petrologic description of the facies is based on total grains, total clay, grain-size, porosity and permeability parameters. The total grain content is the sum of the quartz, feldspars, mica and heavy minerals from the modal analyses. The grain size is expressed as the average diameter in millimeters of ten representative

grains of a thin section. The total clay content is from the XRD-analyses and also includes the mica content of the samples.

Facies A: Massive sandstones

The term massive sandstone is used variously in the literature on deep-water deposits (e.g. Stow & Johansson 2000). In our study, massive sandstones occur as both amalgamated (subfacies A1, Figs. 3, 4a) and interbedded (subfacies A2, Figs. 3, 4b) medium to coarse-grained sandstones with a dominant structureless, massive appearance. Some of the massive sandstones are deformed by water escape. To document any differences in reservoir quality caused by water escape, we introduce subfacies A3 (Figs. 3, 4c) for massive sandstone with water escape structures.

Subfacies A1: Amalgamated massive sandstones

Description. - This facies consists of massive amalgamated matrix-poor sandstones (Figs. 3, 4a). The individual beds are typically up to 1 m thick, with amalgamated units up to more than 10 m thick. Beds normally have sharp bases, (commonly erosive) cutting underlying laminae, or are continuous but squashed (loaded) and have an undulating surface. The beds are generally non-graded, although faint top normal grading occurs with occasional thin intervals with ripple and/or convolute lamination. Inverse grading is occasionally observed in the lower most part of individual beds, however, the overall grain-size distribution is uniform with generally medium to occasional coarse to granular grain sizes (Fig. 3). Rounded green mud clasts may occur at the base, or within these beds, often marking surfaces of amalgamation. Deformation structures due to water escape are common. These structures are grouped and described in subfacies A3.

Interpretation. - The degree of amalgamation is normally a function of the time between emplacements of successive beds, or is caused by the erosive nature of the sandstone bases related to local scouring of the flows. The undulating and squashed character implies loading of the newly deposited sediments onto the underlying water-rich sediment. Due to the faint grading, erosive character, coarse grain-size, matrix-poor nature and associated water escape structures, the facies is interpreted as having been deposited by a high-density turbidity current according to the descriptions and definitions of Lowe (1982). Rapid deposition forming thick sandstone beds probably reflects the beginning of lateral expansion of flows from a channelized setting, or filling of pre-existing channels by large sandy flows.

Subfacies A2: Interbedded massive sandstones

Description. - These sandstone beds are very similar to those described in subfacies A1, but differ in being thinner and interbedded with mudstones (Figs. 3, 4b). Like subfacies A1, these beds are coarse-grained and some are weakly graded with a thin rippled top. The top of the beds is commonly sharp with thin mudstone interbeds occurring between the sandstones (Fig. 4b). These mudstones range from almost entirely clay, to others with a high proportion of silt.

Interpretation. - The sandstones are, like subfacies A1, interpreted as high-density turbidites, but were deposited with less frequency. The presence of mudstones between sandstones indicates time intervals between the emplacement of successive flows. The sharp tops indicate relatively rapid deposition with transport of the remaining suspended sediment further down slope.

Subfacies A3: Dewatered massive sandstones

Description. - Subfacies A3 is introduced to illustrate the differences in reservoir quality between beds with or without fluid escape structures. Fluid escape structures occur in both massive sandstones of subfacies A1 and A2, but the structures are most common in beds thicker than 40 cm. Two types of fluid escape structures are observed: curved concave-upwards dish structures and vertical pillars (see Lowe 1975 and Figure 4c). The pillars, normally a few millimeters to 1 cm in width, are paler in color and cleaner in texture than the surrounding sandstone (Fig. 4c).

Interpretation. - Evidence of fluid escape structures implies deposition from a flow that deposited sand so rapidly that abundant fluid was initially trapped between the grains. This implies the presence of large volumes of fluid in the initial deposit and transportation by a turbulent flow. In the earliest stages of bed compaction (probably during deposition of higher parts of the same bed), the excess fluid escaped upward, and formed pipe and dish structures. Dish structures preferentially develop if the beds have crude stratification with slight vertical variation in permeability (Lowe 1975). The upward escaping water may be forced to flow horizontally for a few cm before escaping through a less permeable layer. The vertical fluid escape pillars form when finer material and water rice upwards out of the sandstone bed (Lowe 1975).

Petrography of facies A

A total of 183 samples of facies A were analyzed by X-ray diffraction or modal analysis. Most of them are from amalgamated sandstones A1 (64) and interbedded massive sandstones A2 (65), while fewer of the analyzed samples represent liquefied amalgamated sandstones A1/3 (20) and liquefied interbedded massive sandstones A2/3 (34). Total grains range from 48-82% of the total volume. Most samples are medium-grained, but range from fine to very coarse-grained. The total clay content is in the range of 8-26% for most samples (Fig. 5). A few sandstones (from the Agat area Fig. 1) have clay-coated grains. These will be further described in the discussion chapter.

There are no significant differences in grain-size distribution within the different subfacies of the massive sandstones. Still, the amalgamated sandstones (A1) contain slightly more grains and less total clay than the interbedded massive sandstones (A2). Subfacies A1/3 and A2/3 have slightly less total clay content than A1 and A2 (Fig. 5).

Porosity/permeability of facies A

A total of 1601 porosity measurements and 1493 permeability measurements were available from facies A; most of the analyses were from subfacies A1 and A2. The porosity curves of A1 and A2 are rather similar (Fig. 6a). About 50% of the samples have porosity values in the range 15% to 30%, with a median porosity of 25%. The liquefied subfacies (A1/3 and A2/3) are slightly more porous than the other two (A1 and A2).

The permeability of facies A is slightly more variable than the porosity (Fig. 6b). The A2 subfacies has more samples with permeability less than 10 mD than the other subfacies, and the A2/3 subfacies has the highest percentage (~53%) of samples with permeability higher than 100 mD. Figure 6c shows the depth distribution of the different facies. Note that facies A1 is more frequent in the deeply buried sediments.

Facies B: Graded and laminated sandstones

Facies B is divided into two subfacies: B1: graded sandstones and B2: cross-laminated sandstones.

Facies B1: Graded sandstones

Description. - Facies B1 is interbedded, graded, finer grained and thinner bedded than facies A (Fig. 3). The facies includes sharply based, normally graded fine- to medium-grained sandstone beds, interbedded with mudstones (Fig. 7a). The beds are generally 5-20 cm thick and are often normally graded with a partly to fully developed Bouma sequence (Fig. 7a). The beds are amalgamated in places, but rarely exceed 1 m in thickness.

Interpretation. - Due to the grain size, grading and the observed Bouma sequences, these sandstone beds have been interpreted as classical turbidites. Interbedding with mudstones indicates a time interval between the emplacement of successive flows.

Facies B2: Cross-laminated sandstones

Description. - This facies includes thin beds of fine- to medium-grained sandstones with well developed planar to cross-lamination (Figs. 3, 7b). Cross-laminated sandstones are rare, but are observed in wells like

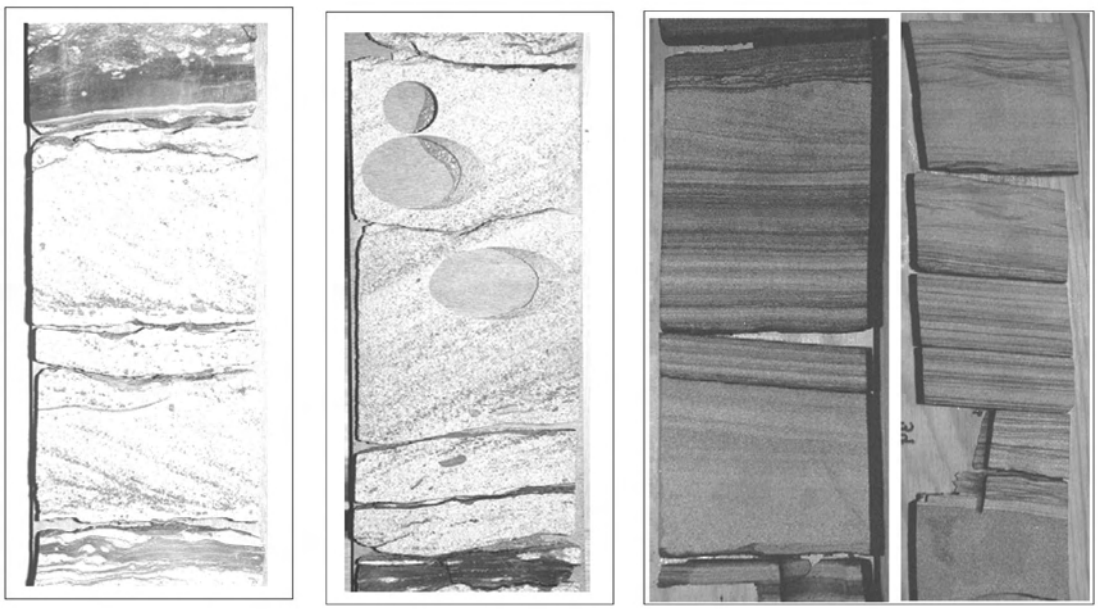

Fig. 7. Core photos of the Facies B
a) Subfacies B1: Interbedded graded sandstone. Left; mainly Bouma divisions b and c. Right; mainly Bouma divisions a, b, c and d. From the Agat area.
b) Subfacies B2: Interbedded cross-laminated sandstone. Left: One set of cross-lamination about 20 cm thick. Right: glauconitic sandstone. Note two cross-laminated beds and interbedded mudstone partings. Both photos from the Lysing Formation, well 6506/12-2, Halten Terrace. Core is 10 cm wide.

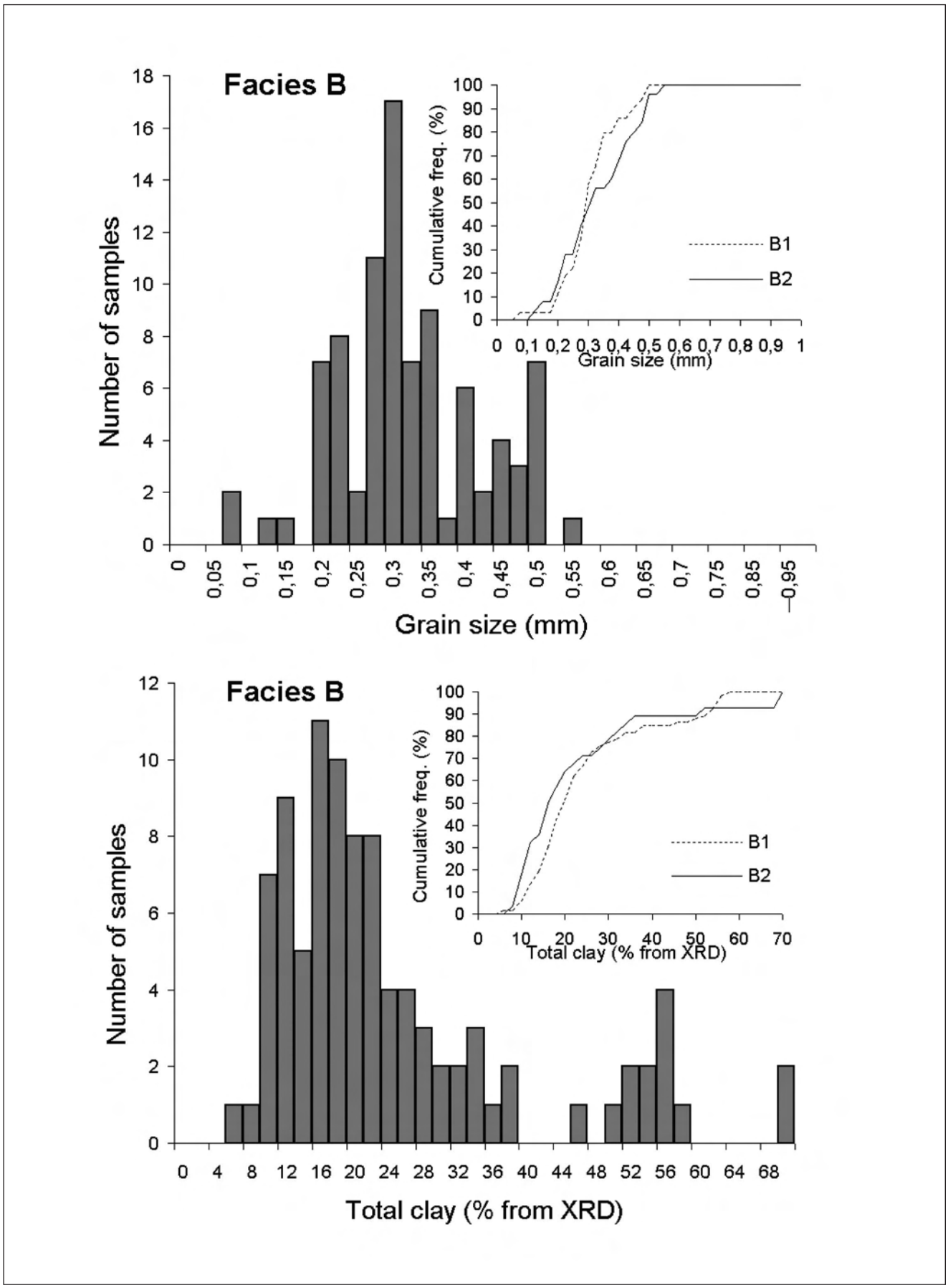

Fig. 8. Petrology of Facies B with grain size distribution and total clay content. Curves in upper right corners show the cumulative frequency of grain size and total clay content, separated by the subfacies B1 and B2.

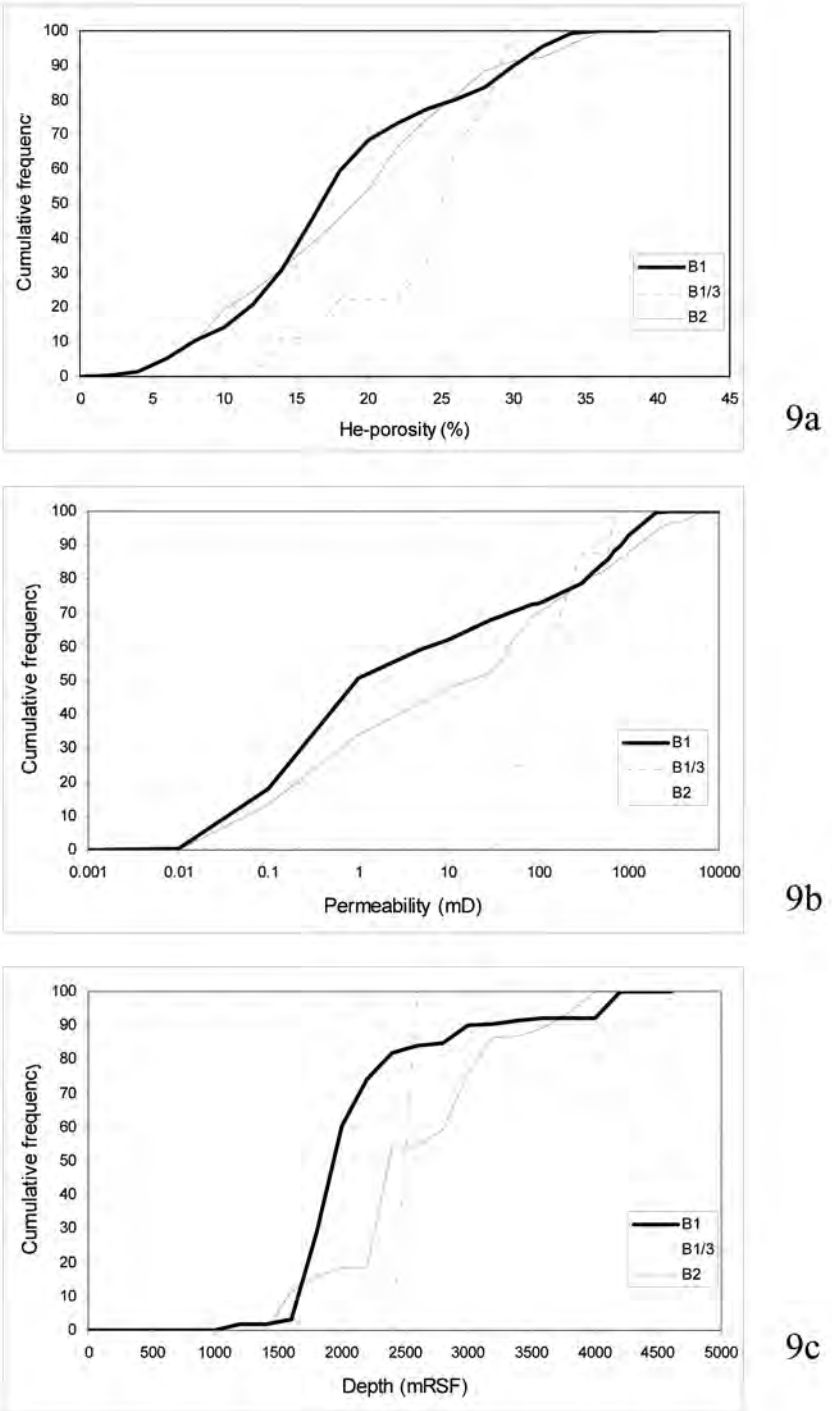

Fig. 9. Cumulative frequency of the Porosity and Permeability of Facies B. Note B1/3 is subfacies B1 deformed by fluid escape.
a) Porosity of facies B
b) Permeability of facies B
c) Burial depth of facies B

6506/12-5 (Lysing Formation on the Halten Terrace, Fig. 7b) and in well 6610/3-1 (Lysing Formation in the Vestfjord Basin, Fig. 1). The cross-lamination occurs in sets about 2-10 cm thick, and glauconite grains often line foresets (Fig. 7b). The cross-laminated beds have a grain size that ranges from upper fine to medium, rarely up to lower coarse, and they are normally interbedded with mudstones. The mudstone partings and interbeds are often dark and clay-rich, and occur below, within and above the cross-laminated sandstones (Fig. 7b). No wave ripples or unambiguous tidal influences are observed. In addition, trace fossils infer deep-water conditions similar to observations from facies A and B1 (e.g. *Chondrites, Zoophycos and Helminthopsis*).

Interpretation. - The cross-laminated glauconitic sandstones from well 6506/12-5 have been discussed and interpreted in different ways during recent years. A tidally influenced environment was suggested by Shanmugam et al. (1994), while Walker & Martinsen (1999)

interpreted this facies to be deep-water deposits organized into a succession of rapidly deposited sandstones alternating with mudstones. As suggested by Walker & Martinsen (1999), the lamination indicates a tractional current, and the beds can be interpreted to be the basal parts of turbidity current deposits. The shear from the overriding turbidity current creates a tractional current, which deposits the coarsest grains. According to Ashley (1990), turbidity currents can create dune forms if the grain size is upper-fine or coarser, and if the velocity is high enough and the currents persist as long as the overriding turbidity current continues to bypass. Several bypassing flows may leave behind thin "lags" of coarse cross-laminated sandstone with preserved interbedded hemipelagic mudstones representing the final muddy fall out from the suspended cloud after bypassing of the main sand portion. Confinement in a channelized setting would help the flows to be sustained to create the cross stratification, but this cannot be proven in the present case.

Petrography of Facies B

A total of 94 samples of facies B were analyzed by X-ray diffraction or modal analysis. 66 samples are graded sandstones (B1), while 28 samples are from laminated sandstones (B2).

Total grains range from 52-68% with a median value of 61%, but there is a cluster of samples with only 40-48% of such grains. The grain sizes range from very fine to coarse, but the majority of the samples are fine or medium-grained. The total clay content range from 6-40%, but there is a cluster of samples with clay contents that range from 52-60% (Fig. 8).

There are no significant differences between the two subfacies regarding total grains and grain size. But the cluster of samples with high total clay content is dominated by facies B1, and nearly all the samples are from the Ormen Lange wells 6305/5-1 and 6305/7-1.

Porosity and permeability of Facies B

Figure 9 shows porosity and permeability curves of facies B. About 70-75% of the measurements are from B1 with a few measurements from B1/3, while the rest (25-30%) are from B2. The porosity values of facies B1 and B2 range from 5-25%, while the porosity of facies B1/3 ranges from 12-30% (Fig. 9a). The permeability ranges from 0.01 mD to more than 1000 mD for facies B1 and B2 (Fig. 9b). Facies B2 has more samples with permeability values higher than 1mD (65%) while only 50% of the B1 samples have permeability values higher than 1mD. The permeability for facies B1/3 is in the range 30mD to 800mD and 50% of the samples have permeability values higher than 100 mD. The burial depth of the B1/3 samples is ~2500m while the burial depth of facies B1 and B2 ranges from approximately 1500-4000m. Facies B1 and B2 have about the same percentage (~10%) of samples buried deeper than ~3250m, but ~45% of the B2 samples are buried deeper than 2500m. Only 15% of the facies B1 samples are buried deeper than 2500m (Fig. 9c).

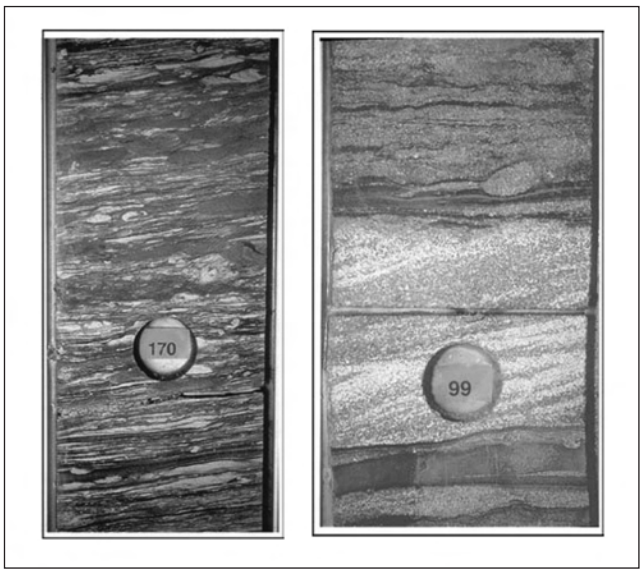

Fig. 10. Left: Heterolitics, bioturbated sandy siltstone with thin rippled layers representing reworking by bottom currents or low-density turbidity currents. Lange Formation, well 6505/10-1, Vøring Basin. Right: Heterolitics, thin cross-laminated sharp-based sandstones. Probably represent deposition by low-density turbidity currents, or reworking by ocean bottom currents. Lysing Formation, well 6505/10-1, Vøring Basin. Core is 10 cm wide.

Facies C: Heterolithic sediments

Description. - The sediments grouped in the heterolithic facies are thin sandstone beds interbedded with dominantly grey to dark grey mudstones with variable degrees of bioturbation (Figs. 3, 10). The number of sandstone beds varies, but they are usually less than 10 cm in thickness, with a very fine- to fine grain size. They have gradational to sharp bases and gradational tops. Low-amplitude ripple cross lamination occurs in this facies (Fig. 10)

Interpretation. - The dark grey and grey mudstones are interpreted as pelagic and hemipelagic deposits in a setting well below storm wave base. The thin graded sandstone beds represent the distal deposits of dilute turbidity currents. The rare low-relief ripple cross-laminated structures (Fig. 10) suggest a slow current able to roll grains along the bed, but not strong enough to create high amplitude ripple cross lamination. This current may have been a sustained basinal current reworking previously deposited sediments. Its genesis in a Cretaceous time period without polar ice-sheets is enigmatic. Present contour currents are driven by tem-

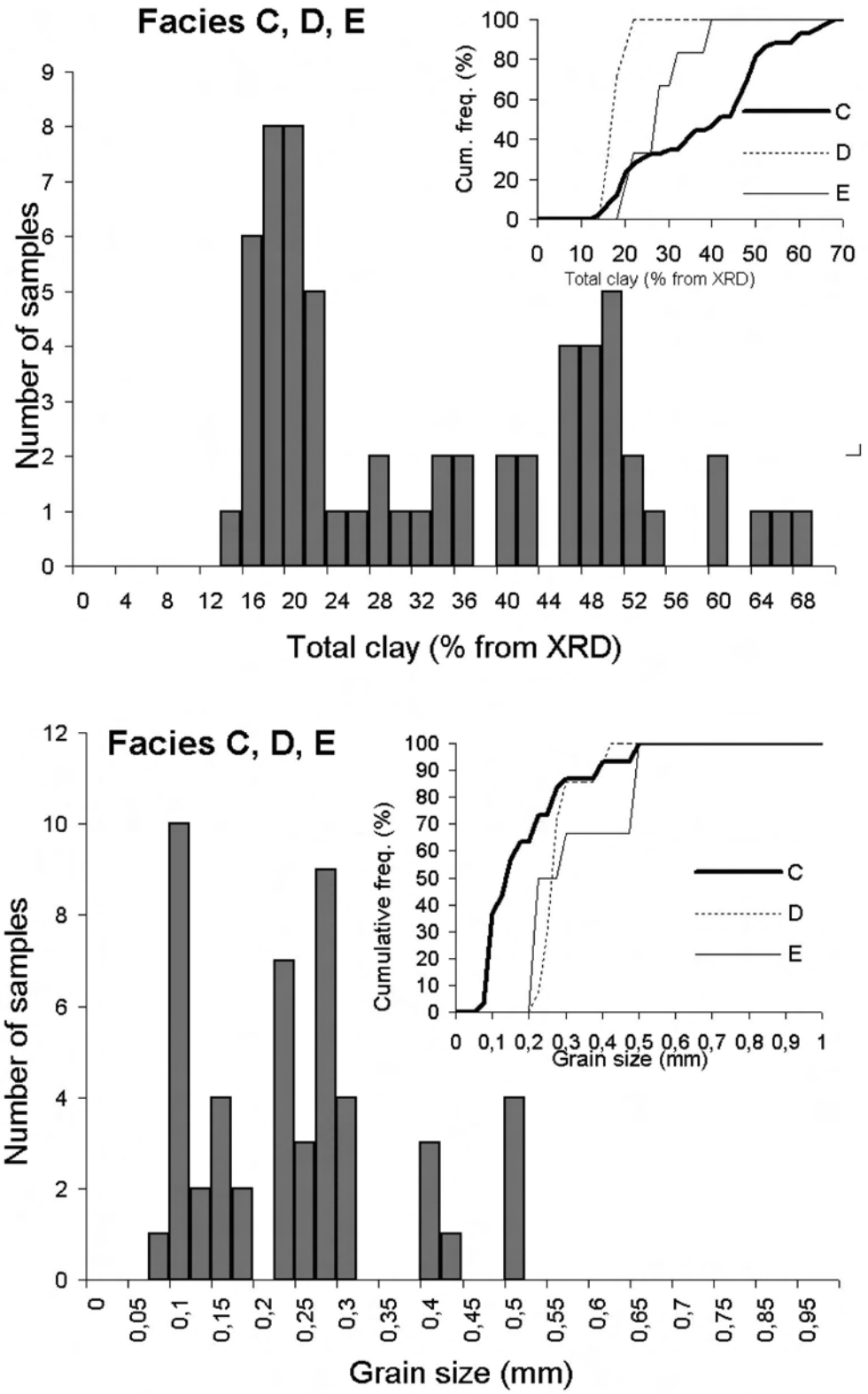

Fig. 11. Petrology of Facies C, D and E with grain size distribution and total clay content. Curves in upper right corners show the cumulative frequency of grain size and total clay content, by the individual facies C, B and E.

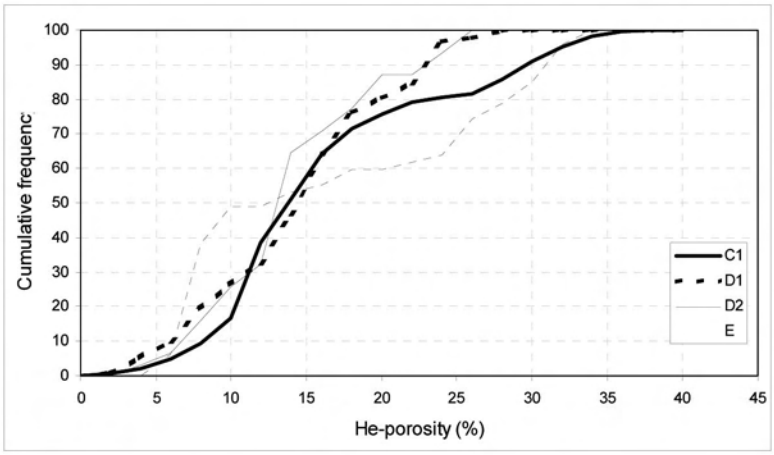

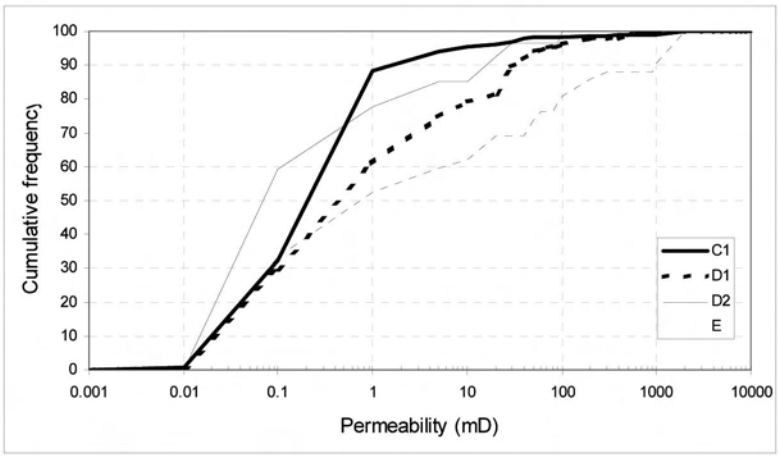

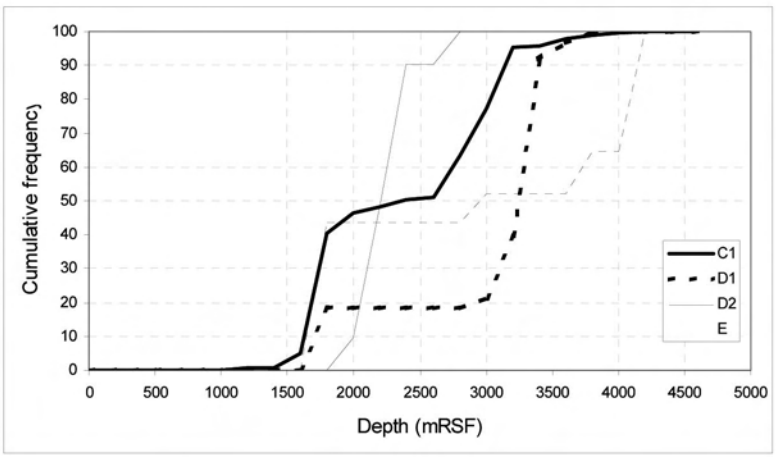

Fig. 12. Cumulative frequency of the Porosity and Permeability of Facies C, D and E

a) Porosity of facies C, D and E
b) Permeability of facies C, D and E
c) Burial depth of facies C, D and E

perature differences in the water column, which are unlikely to have existed in the Cretaceous basins offshore Norway. A relatively narrow seaway configuration between mainland Fennoscandia and Greenland prior to seafloor spreading in the early Eocene may have set up such a current, but further research is needed to fully explain the current's origin. Facies C was probably deposited in an outer/distal fan environment, which was influenced by low-velocity basinal currents.

Petrography of Facies C

A total of 43 samples of facies C were analyzed by X-ray diffraction or modal analyses. Total grains range from 30-68% with a median value of 45%, the grain size is fine-grained for most of the samples, but some medium-grained samples are also classified as facies C (Fig. 11). The total clay content ranges from 12-68% (Fig. 11). Most samples from this facies are from the Ormen Lange well 6305/1-1 T2.

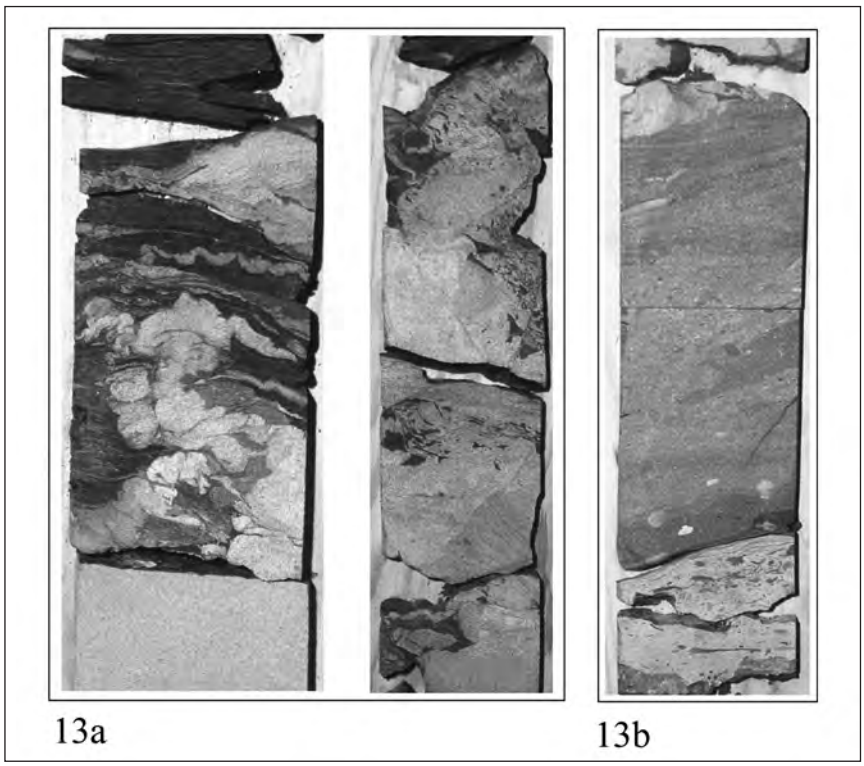

Fig. 13. Core photos of the Facies D
a) Facies D1: Deformed sandstone, sandstone dykes injected upwards into dark mudstone. Lange Formation, Agat area.
b) Facies D2, transitional to facies E: Deformed sandstone, original poorly sorted bed, possibly transported by debris flow (facies E) deformed by gravitational sliding and some sandstone injection. Lange Formation, Agat area. Core is 10 cm wide.

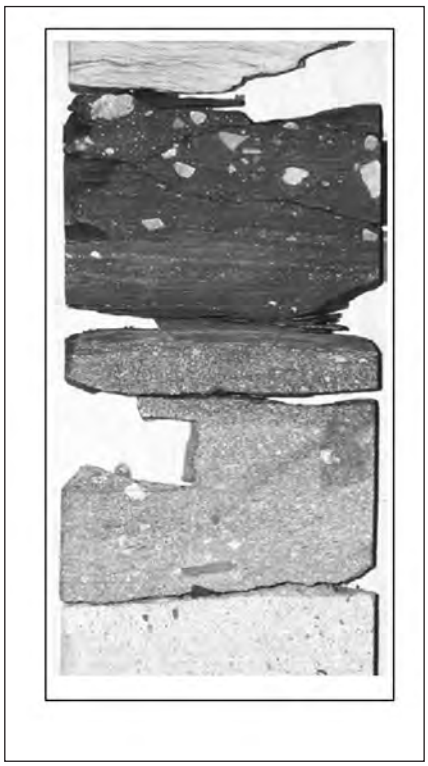

Fig. 14. Core photos of the Facies E: Debris flow, note dark, mud-rich bed with inverse graded, large floating subangular clasts. Lange Formation, Agat area. Core is 10 cm wide.

Porosity and permeability of Facies C

The porosity values are in the range 5-35% (Fig 12a). Although the permeability values range from less than 0.1 mD to ~1000 mD, only 10% of the measurements have permeability values higher than 1 mD (Fig. 12b). The burial depth varies from ~1500-4000m, but only 25% of the measurements are from samples buried deeper than 3000 m (Fig. 12c).

Facies D: Deformed sediments

Deformed sediments (Facies D) are divided into two subfacies D1 (injected sandstones) and D2 (slides and slumps).

Subfacies D1: Injected sandstones

Description. - Sand dykes, sand sills and complexly deformed sandstones and mudstones are characteristic of this facies (Figs. 3, 13a, 13b). Dykes are normally injected upward from the top of a sandstone bed into the overlying mudstone. Sills have a sub-horizontal attitude and clearly crosscut the stratification in the mudstone. Sand injected into sand is common. Several features are indicative of remobilization of the sands. These are: deformation and unusual crosscutting relationships between bedding planes or lamination, and bed bases that are very irregular or wavy and show local injection from the base upwards (Figs. 13a, 13b).

Interpretation. - Both dykes and sills imply that nearby sandstone was buried whilst containing significant amounts of pore water. The intrusion of sand into the surrounding sediments implies liquefaction of the sands and remobilization where bodies of poorly consolidated sands encased in a fine-grained hemipelagic succession, were subjected to liquefaction and remobilization as a result of building up of overpressure (Hiscott 1979). A seismic shock or collapse of the overpressure will eventually pump fluids and unconsolidated sands through the fault and joint system.

Subfacies D2 - Slides and slumps

Description. - Slides and slumps are rare in the cored sections. A 5 m thick slide of Albian age is described in well 35/9-3T2. The deposits, mainly consisting of low-density turbidite sands, are rotated and mildly deformed. The deformation is associated with the slope on a levee setting close to a turbidite channel. Slumps described in well 6204/11-1 (Lange Formation) are transitional to debris flows (facies E), and are dominated by

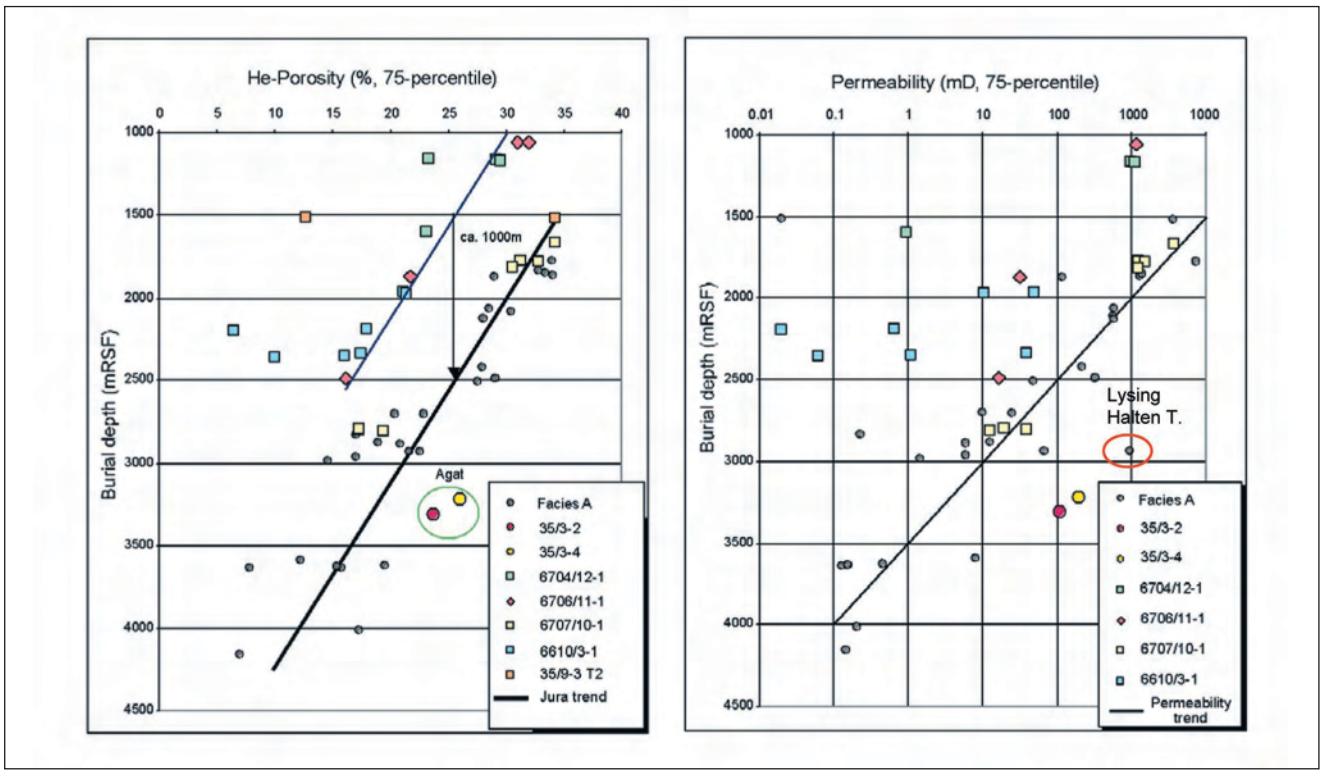

Fig. 15. Porosity and Permeability of Facies A plotted against burial depth. The solid line represents the Jurassic trend line from shallow-marine clean sandstones with less than 20% clay from Ramm (2000). The porosity of most of the wells analyzed in this study seems to follow the same trend. However, the 75th percentile porosity from some wells (6610/3-1, 6706/11-1 and 6704/12-1) differs from the trend. Note also the relative high values for the Agat wells. These are considered to be related to clay coating preventing quartz overgrowth, and are also a function of sediment source area. The permeability plot shows trends similar to the porosity plot, with low permeability associated with the low porosity wells, and high permeability associated with the high porosity wells.

pebbly mudstones. In the wells 6610/3-1 and 6609/5-1, thin intervals (a few meters) of thin turbidite sandstone beds are mildly deformed and folded.

Interpretation. - Sliding and slumping are down slope displacement of a semi-consolidated sediment mass along a basal shear plane while retaining some internal (bedding) coherence. The degree and style of internal deformation varies with position in the moving layer and with the strength and heterogeneity of the slumping/sliding material. Where observed in the cores from the present study, the slides are interpreted to reflect primary deposition from turbidity currents, and later affected by short distance rotational sliding commonly associated with channel margins. The slumps have higher internal deformation and are transitional to the definition of debris flows (facies E, Figs. 13b, 14). These indicate longer transport distance, and those observed are associated with mudstone content and higher gradient slopes.

Petrography of Facies D

Only 14 samples from this facies were analyzed by X-ray diffraction or modal analyses. Eleven samples are from injected sandstones (D1) and 3 are from slides/slumps (D2). Nearly all the samples are from the Agat wells in block 35/3 in the northern North Sea. The total grain content is in the range 54-76%, and the grain size ranges from 0.2-0.3 mm (fine/medium). The total clay content is in the range 14-22% (Fig. 11).

Porosity and permeability of Facies D

The majority of the measurements are from subfacies D1. The porosity values are in the range 5-25% with a median porosity value of 14% for D1 and 13% for D2 (Fig. 12a). The permeability values range from less than 0.1 Md-~100 mD, and ~40% of the D1 measurements have permeability values higher than 1 mD while only 20% of the D2 measurements have permeability values higher than 1 mD (Fig. 12b). The burial depth is mainly in the range 2000-2500 m for measurements from facies D2. The D1 measurements are from samples located at burial depths between ~1500-3500 m with 80% of the measurements being from samples buried deeper than 3000 m (Fig. 12c).

Facies E - Debris flows

Description. - Interpreted debris flow deposits are rare in the cored intervals. They occur both as poorly sorted

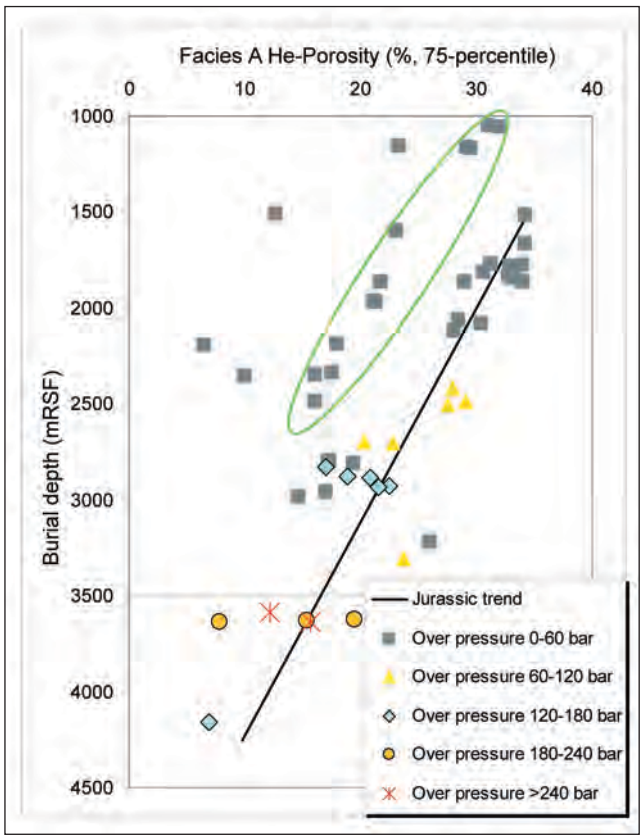

Fig. 16. Porosity of Facies A plotted against burial depth and estimated overpressure (bar overpressure). Although data are limited there are no obvious trend suggesting better porosity in wells with present day high overpressures compared to normal pressured reservoirs. Green circle around low porosity values relates to sediments exposed to late structural uplift and/or higher subsurface temperatures (see Fig. 15).

mud-rich sandstones with disorganized scattered sub-angular mud clasts (occasionally outsized), and as pebbly mudstones (Fig. 14). Isolated beds, or stacked units up to a few meters thick are described from wells like 6204/10-1 (Lysing Formation), 6607/5-2 (Nise Formation) and 6406/2-3 (Lange Formation). These are sandy with scattered, disorganized, sub-angular outsized mud clasts (up to 8 cm) and occasionally sandstone blocks. The beds are in general massive, poorly sorted and have non-erosive bases. Stratification and internal grading of grain-size are rare, but inversely graded pebbly mudstones are observed (Fig. 14).

Interpretation. - The large outsized, sub-angular mud clasts are disorganized and indicate a short transport distance. The mud-rich composition suggests deposition with a high cohesive strength. The poor sorting, lack of stratification, lack of grading, chaotic fabric and non-erosive bed bases all indicate non-turbulence and deposition as debris flows (Middleton and Hampton 1976). Most of the described debris flow deposits were probably due to short-lived events derived from a nearby collapsing channel margin. The mudstones are broken up and incorporated into the sandstones. Depending on the gradient and flow distance, the moving layer will deposit quickly or accelerate and transform into a more dilute flow such as a turbidity current. Facies E is often described in association with turbidite channel fill (channel margin collapse) or with submarine slopes.

Petrography of Facies E

Only 6 samples from this facies were analyzed by X-ray diffraction or modal analysis. The total grain content varies from 42-68%, the grain-sizes are medium and the total clay content ranges from 18-40% (Fig. 11).

Porosity and permeability of Facies E

The porosity ranges from ~5->30%. 50% of the samples have a porosity between 5% and 12 %, and 40% of the samples have porosity higher than 20% (Fig. 12a). The permeability varies from 0.01 mD to over 1000 mD, with a median permeability value of 1 mD (Fig. 12b). The burial depth ranges from ~1500m to over 4000m and 50% of the measurements are from samples buried deeper than 3500m (Fig. 12c).

Petrographic variations between the facies

Lithological variations

Facies A has more total grains, slightly coarser grain-size and less total clay than facies B (Figs. 5, 8). Subfacies A1 has more total grains, less total clay and similar mean but a narrower spread of grain size than subfacies A2 (Fig. 5). Subfacies A1/3 (subfacies A1 deformed by fluid escape) and A2/3 (subfacies A2 deformed by fluid escape) have no significant differences in composition than the respective subfacies A1 and A2, other than a slightly less total clay content (Fig. 5). Subfacies B2 has a similar grain size but slightly less clay than subfacies B1 (Fig. 8). Facies C has a wide range in total grain content, a general high clay content, and the average general grain size (0,1-0,15 mm) is less than in the other facies (Fig. 11). Facies D (few data) has a composition similar to facies B (Figs. 5, 11), whereas Facies E (very few data) has a relative high total clay content and a wide range of grain sizes (Fig. 11).

Porosity and permeability variations

Samples from facies A have slightly higher porosity and permeability than samples from facies B (Figs. 6a, 9a). A1 has similar porosity values as A2 (Fig. 6a), but is more commonly subject to deeper burial (Fig. 6c), suggesting higher porosity at similar burial depths. Subfacies A1/3 and A2/3 have slightly higher porosity and

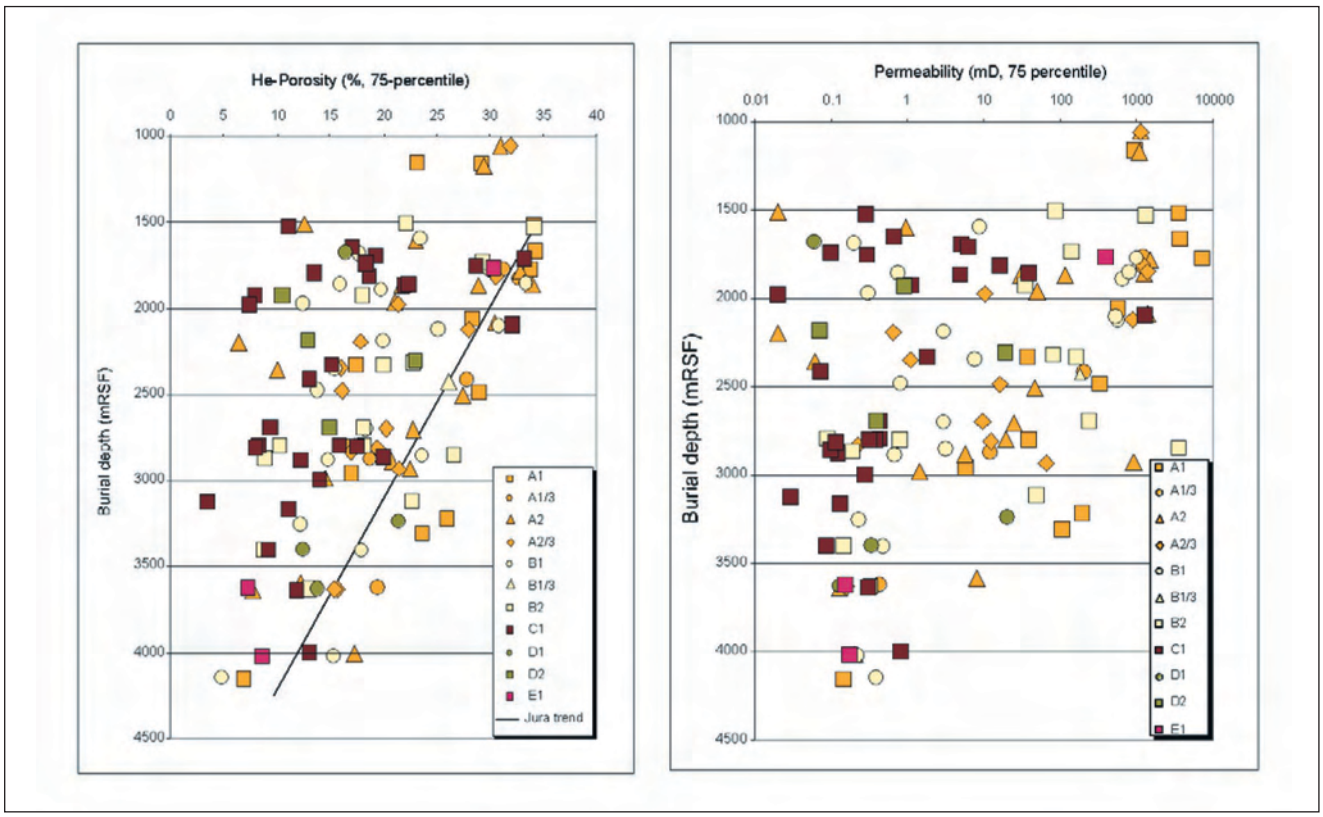

Fig. 17. Porosity and permeability vs. burial depth plotted by depositional facies.

permeability than A1 and A2 respectively (Figs. 6a, 6b). Subfacies B2 has slightly higher porosity and permeability than subfacies B1 (Figs. 9a, 9b). Samples from facies C have the poorest reservoir quality with low permeability values, but relatively high porosity values (Fig. 12a). Samples from facies D and E have a wide range of porosity and permeability values (Figs. 12a, 12b).

Spatial petrographic variability

To analyze and subsequently visualize the spatial petrologic variability, similar facies were plotted against burial depth. Porosity and permeability values for facies A (massive sandstones) fall along two general porosity/depth and permeability/depth trends (Fig. 15). The bulk of the samples from facies A lie along a porosity/depth trend similar to that reported for Jurassic clean shallow-marine sandstones with less than 20% clay by Ramm (2000). We call this trend the "normal" trend. By contrast, facies A sandstones from the wells 6704/12-1 and 6706/11-1 (Vøring Basin) and well 6610/3-1 (Vestfjord Basin) have lower porosity and permeability values for a given depth than do samples from other wells used in this study (Fig. 15).

Wells located on the Dønna Terrace (mainly Lysing and Lange formations sandstones) follow the "normal" trend, but have exceptionally high permeabilities in a few sandstones of the Lange Formation. Similar observations are made in wells located on the Halten Terrace, where the Lysing and Lange formations sandstones follow the "normal" trend, but with exceptional high permeabilities in a few Lysing Formation sandstones (Fig. 15). However, the wells located in the Agat area (Figs. 1, 15) show exceptional high values of both porosity and permeability of Facies A in the Lysing Formation sandstones. The wells in the Møre Basin penetrate Tang and Springar formations sandstones; and follow the "normal" quality trend towards burial depth.

These observed spatial differences in reservoir quality for one facies at similar sediment burial depths show the complexity involved in predicting porosity and permeability in immature explored areas. As discussed below, the differences in reservoir quality observed in facies A can probably be related to variations in temperature history and the nature of the sediment source area.

Discussion

To what degree do fluid pressure, depositional processes, sediment source area and temperature history control the reservoir quality of the studied deep-water sandstones?

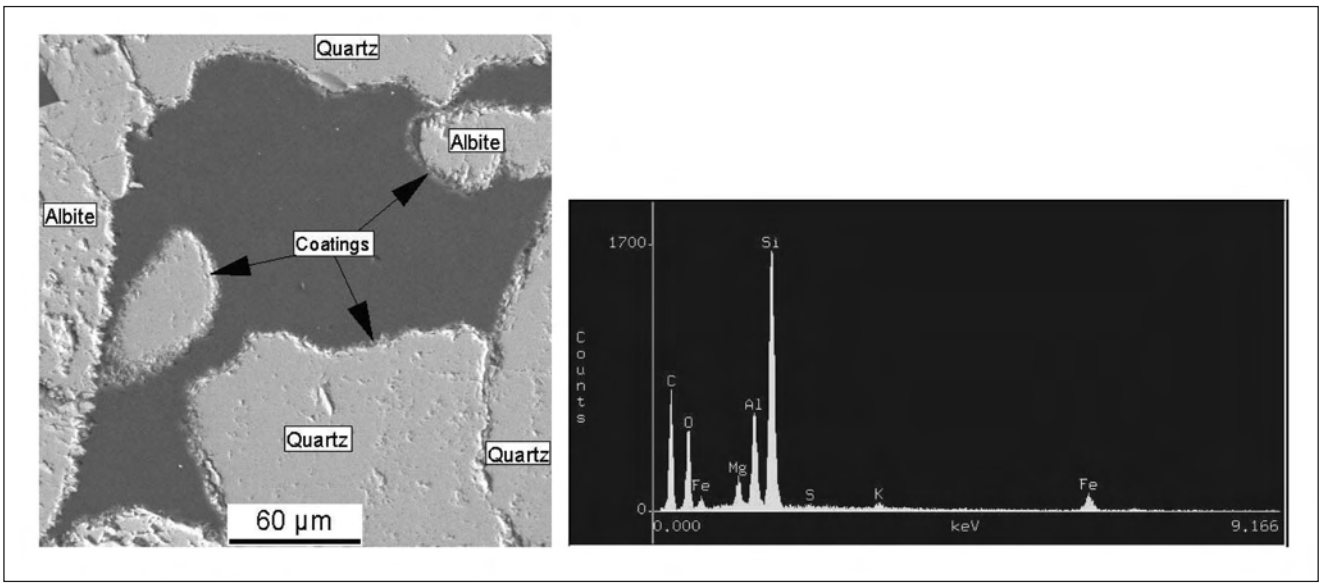

Fig. 18. Left: Scanning electron microscope (SEM) photo of coating on grains in sandstone of Facies A in well 35/3-2 (Agat) at 3602.02 mRKB. Note the lack of quartz cement and the variable thickness of coating and its occurrence at the grain contacts. Right: Spectra of the clay coating material in photo, showing a chlorite/smectite composition.

Fluid Pressure

Estimation of the effect of fluid overpressure in the reservoirs is problematic due to the complexities in estimating the timing of the pressure and burial history. However, based on the fluid pressure estimates, no unambiguous correlation is observed between overpressure and porosity or permeability (Fig.16). Samples from reservoirs with high present day overpressure do not appear to have consistently higher porosity and permeability values than samples from reservoirs with minor to no present day overpressure. Based on the data available, high fluid overpressure has not improved porosity preservation compared to the normally pressured sandstones of similar facies at similar burial depth. However, the database is limited, and there are several factors influencing this relationship. A complicating factor is timing of fluid overpressure; shallow emplacement would have had a better potential for preserving the reservoir quality than late emplacement (Bloch et al. 2002).

Depositional process

As shown in Figure 17, porosity and permeability for a given depth vary significantly with facies. Based on a detailed facies and petrologic analysis, the following general observations can be made:

- Sandstone with larger grain-size and lower total clay content, has higher porosity and permeability for a given depth than finer grained more clay-rich sandstone (Facies A is better than B is better than C).
- Sandstone with the highest clay content has the lowest permeability values, suggesting that clay content is a major control of the permeability (Subfacies A1 has higher permeabilities for a given depth than samples from subfacies A2, subfacies B2 is slight better than B1 and facies C, the most clay-rich facies, has the lowest permeability values).
- Dewatering of sandstones seems to result in slightly higher porosity and permeability, possibly by removing (or concentrating) clay from the host sediments (Subfacies A3 has less total clay and slightly higher porosity and permeability than samples from subfacies A1 and A2).
- Deformed sandstones (by gravitational sliding or injection) seem to have compositions similar to the "host" sediments, although the injected sandstones have slightly poorer quality than the undeformed facies A.

The sediment transport process primarily controls variation in grain size and clay content in sandstone in the study area. High-density turbidites (facies A) deposited coarser grain sizes and sand with low clay content (the finer grained sediments were in suspension and were deposited during the waning phase and classify as low density turbidites of facies B or C). These high-density turbidites were water-rich, often rapidly deposited and some of the beds experienced water escape during (or soon after) deposition. The de-watering appears to have reduced the clay content of these sands, and further enhanced the reservoir quality.

Facies B2 (cross-laminated sandstones) has slightly better porosity and permeability than facies B1 (graded sandstones). The stronger, sustained currents acting during deposition of B2 sorted the sediments and pus-

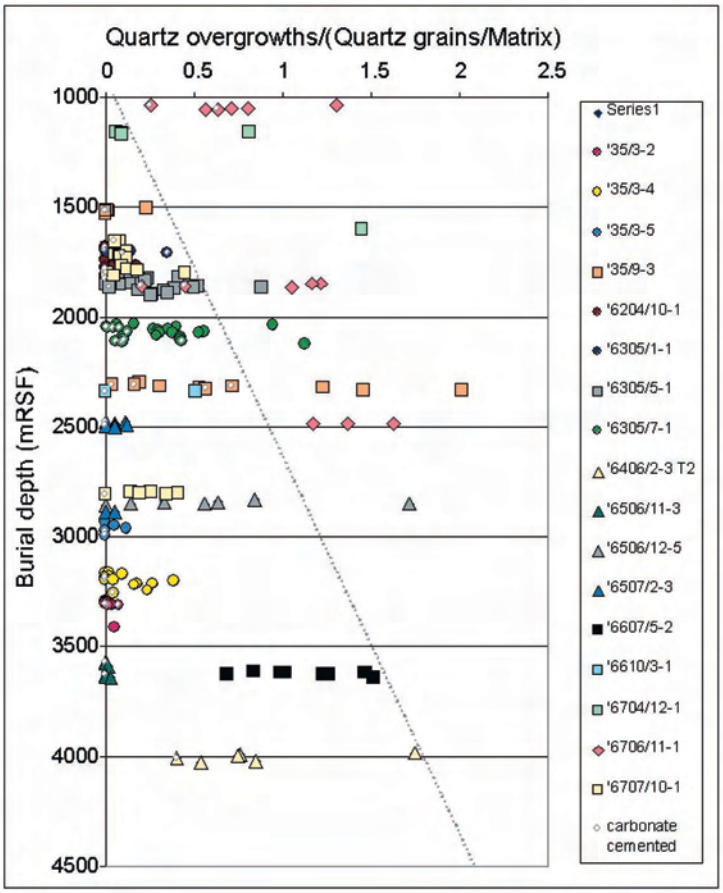

Fig. 19. Quartz overgrowths vs. burial depth of facies A. The diagram shows how the ratio of quartz overgrowths to macro porosity increases with increasing burial depth. All the samples have less then 10% of point counted matrix. Quartz overgrowths tend to nucleate on quartz grains and grow into macro pores, and the amount of quartz overgrowth increases with increasing temperature (burial depth). The amounts of macro porosity decrease with increasing burial depth due to mechanical compaction and to cementation. The grey line indicates the expected maximum-ratio for a given burial depth. Wells with a ratio much higher than this line were probably exposed to temperatures higher than the present burial depth would suggest, whereas wells with a ratio much lower than this line have been exposed to lower temperatures, or contain grain coating clays that prevent precipitation of quartz overgrowths. Note the relative high quartz overgrowth values in wells 6706/11-1 and 6704/12-1, but low values in well 6707/10-1 and correspondingly low and high porosity and permeability values in figure 15.

hed the clay into suspension. The final deposits were better sorted and have fewer fines than the low-density turbidites of Facies B1.

Samples from facies C are characterized by high porosities and low permeabilities (Figs. 12a, 12b), The high porosities can be attributed to abundant microporosity associated with the relatively high clay content (Fig. 11). Microporosity is fairly ineffective for fluid flow resulting in lower permeability for a given porosity of facies C samples than is shown by samples from other facies.

The injected sands (subfacies D1) seem to have lower porosity and permeability than the host sediment. During injection, sand and water are squeezed into overlying sediments from the over-pressured water-rich host sediment. The finer material is transported easily, and some may be removed from the host sediments and concentrated in the sills and dykes. In addition, mud fragments are occasionally picked up and incorporated into the sills and dykes during injection.

Source area

Although the depositional processes were the same for similar facies in different areas, there are some major differences regarding the grain size and to some extent the clay content. Average grain size is larger in the massive sandstones from the Møre Basin than in the samples from Agat area and Vøring Basin. The massive sandstones from the Møre Basin also contain slightly more clay. Transport distance and degree of sorting during transport can explain some of these differences. However, these are all facies A transported by high-density turbidity currents, and according to Martinsen et al. (2005) the overall depositional environments for the Ormen Lange and Vøring Basin sandstones are similar, being high net to gross, sheet-like, sand-rich basin floor fan systems. The Agat system is a deep-marine intra slope system and the sandstones are accordingly deposited closer to the sediment source (Martinsen et al. 2005). The samples from the Møre Basin, Vøring and Agat systems have three different sediment source areas, where the Vøring sandstones are sourced from East Greenland, the Møre sandstones from the middle part of Norway and the Agat sandstones from western Norway (Fonneland et al. 2004). It is therefore tempting to suggest that the observed differences in sandstone petrography can be assigned to differences in the sediment source. During the Late Cretaceous and Paleocene, the Vøring Basin drained East Greenland re-

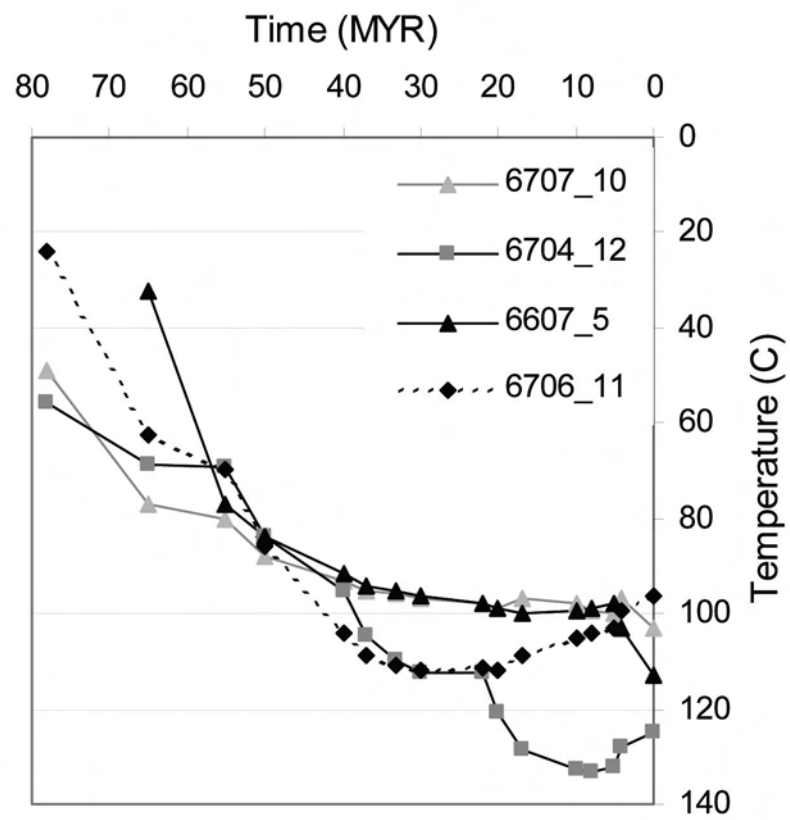

Fig. 20. Burial history temperature curves of wells in the Norwegian Sea. The wells following the "low porosity trend" from Figure 15 (blue 6704/12 and orange 6706/11) have had temperatures higher than 100° C for the last 40myr. The wells following the "normal porosity trend" in Figure 15 (green curve 6607/5 and red curve 6707/10) have only recently exceeded 100° C. This coincides with the observations that the "low porosity" wells contain more quartz overgrowths than the "normal porosity trend" wells at similar depths (see Fig. 19). The burial history temperatures are forward modeled in-house at Hydro using the Petromod 3D basin modeling software including advective as well as conductive heat flow, from the 2D/3D lithospheric code by Zeyen & Fernandez (1994).

depositing Triassic and Jurassic sandstones, while the eastern Møre Basin systems drained the older Norwegian Basement. The Agat sandstones were deposited on the deep-marine slope, and represent re-deposited shallow-marine Cretaceous sediments sourced from western Norway (Martinsen et al. 2005; Fonneland et al. 2004).

A few anomalously high porosity and permeability values are seen in the Agat area, in wells 35/3-2 and 35/3-4 (Fig. 15). These (facies A1) sandstones have clay-coated grains of chlorite/smectite composition that inhibited the nucleation of quartz overgrowth (Fig. 18). Ehrenberg (1993), and Bloch et al. (2002), documented the occurrence of chloritic coats in shallow-marine sandstones on the Norwegian shelf, and these authors concluded that clay-coated grains could preserve reservoir quality during deep burial of shallow-marine sediments. However, the occurrence of clay coats in deep marine settings such as in the Agat area is not well documented in the literature, and the origin of grain coats in deep-water sandstones is poorly understood.

The Agat sandstones have a unique sediment source area, and are re-deposited shelf or shallow marine sediments (Fonneland et al. 2004; Martinsen et al. 2005). Wilson (1992) has described inherited grain-rimming clays in sandstones and identified some criteria for recognition of inherited clays. Our observations of clay coats from the Agat sandstones are similar to those of Wilson (1992). There are variable thickness of the coating and coatings at the grain contacts (Fig. 18). Our suggested interpretation is therefore that the grain coatings are inherited from the shelf- and shallow-marine sediments.

Temperature history

Figure 15 shows porosity and permeability versus burial depth for facies A. Most data show a close to linear decrease in porosity with increasing burial depth. This is defined as the normal porosity trend, which is relatively similar to the trend from the Jurassic shallow-marine clean sandstones with less than 20% clay defined by Ramm (2000). The deviation from the normal porosity trend is about ±4% (Fig. 15). The normal permeability trend is more diffuse but shows a decrease in permeability of an order of magnitude every 500 m, starting with 10.000 mD at 1500 m burial depth. The deviation is less than ±3/4 order of a magnitude (i.e. at 3000m burial depth, the average normal permeability will be 10 mD ranging from 1,5-40 mD).

A trend of significantly lower porosity values for a given depth is shown by samples from wells 6704/12-1 (Gjallar Ridge), 6706/11-1 (Vema Dome) and well 6610/3-1 (Vestfjord Basin) (Figure 15). Facies, lithology

and stratigraphy are similar to the sediments that follow the normal trend (for example, well 6707/10-1, Nyk High), and the differences must therefore be explained by factors other than depositional processes. The low porosity wells have significantly higher quartz cement abundance than similar facies A sandstones at similar burial depths (Fig. 19). As shown in figure 19, the amounts of quartz cement increases with increasing burial depth. This correlation is interpreted to be due to increase in temperature, associated with the increase in burial depth. Barclay & Worden (2000) suggests that quartz cement from the Magnus sandstone in the North Sea may be sourced by feldspar dissolution, which in turn may be related to the input of CO^2 suggesing that the amount of quartz cement is not directly related to temperature. However, Barclay & Worden (2000) limit this type of diagenesis to early oil charging of the sandstones. There are no oil or gas accumulations associated with the sandstones in the "low porosity" wells. It is therefore not likely that the increased amounts of quartz cement observed in our study are due to feldspar dissolution.

The burial history temperature curves (Fig. 20) show that the wells forming the "low porosity" trend (Fig. 15, blue and orange colors) have had temperatures higher than 100° C for the last 40 million years. The wells forming the normal trend (like 6707/10-1) have only recently exceeded 100° C. The higher thermal exposure of samples from the "low porosity" wells is compatible with the observations that these "low porosity" wells contain more quartz overgrowths than the "normal trend" wells at similar depths (Fig. 19). Based on these observations, we suggest that "low porosity" wells have higher quartz cement values due to higher temperature. Taking this into account, two explanations for the low porosity trend are possible: 1) the sediments have been more deeply buried, exposed to higher temperatures and later uplifted, or 2) the subsurface heat flow has been higher in the wells with more quartz cement compared to the other wells.

The low porosity and permeability observed in well 6704/12-1 on the Gjallar Ridge may be caused by high temperatures related to the volcanic margin nearby and associated heat flow from deeper magmatic bodies (Fjeldskaar et al. 2003). Well 6706/11-1 is located on the Vema Dome which was a Cretaceous depocenter inverted during post-breakup compression (Mogensen et al. 2000). The late structural uplift associated with closeness to the Vøring margin can explain the exposure to higher temperatures and thereby the low porosities.
A late structural uplift of about 750-1000 m is suggested as an explanation for the low porosities in the Cretaceous sandstones in well 6610/3-1 (Fig. 15). This uplift is considered to have been related to the regional Neogene uplift of the Fennoscandia (Riis 1996; Hjelstuen et al. 1999).

Conclusions

- The control of reservoir quality in deep-marine systems in the Norwegian Sea is dependent on: 1) the sediment depositional processes 2) source area and 3) temperature and burial history.
- A facies scheme for the deep-marine sediments has been developed. High- and low density turbidity currents are the dominant transportation media, but well preserved reservoir quality occurs in rare cross-laminated sediments transported by strong sustained sea-floor currents.
- Grain size and total clay content have major influences on the porosity and especially the permeability. The high-energy transport processes (high-density turbidity currents and strong sustained sea-floor currents) deposited the coarsest and most clay-poor sediments.
- Dewatering of sediments removed some fines, and gave slightly better reservoir quality in sediments with such structures.
- Sandstone sills and dykes transported fines during injection, and have slightly poorer quality than their host sediments.
- Clay coating on grains produced in a shallow-marine source area was locally preserved during redeposition and gave anomalously high qualities by inhibiting quartz cementation.
- The majority of the sandstones examined in this study follow porosity/depth and permeability/depth trends (defined as "normal" trends) similar to the trend from the shallow-marine Jurassic sandstones reported by Ramm (2000). The high-density turbidites (Facies A) have a porosity range of 4 porosity units, and permeability range of 3/4 of an order from the "normal" trend. The low-density turbidites have a porosity range of 5%, and a permeability range of one order from the "normal" trends.
- In the Cretaceous and Paleocene intervals in wells in the Norwegian Sea, there is no obvious relationship between overpressure and porosity. However, this can be explained by relatively late emplacement of the overpressure in the study area.
- Sedimentary rocks in the Vøring Basin that experienced higher thermal exposure than other wells in this study have greater quartz cement abundances and poorer reservoir quality than similar facies at similar burial depths elsewhere in the study area.
- Reservoir quality variations across the study area reflect the complex interplay of sandstone composition and texture (controlled by depositional processes and source area) and burial history (temperature and burial depth history) in controlling reservoir quality. By considering all these factors, regional reservoir quality studies can both aid in the prediction of sweet spots with high-quality reservoir sandstones, and help identify areas with anomalous temperature or burial history.

Acknowledgements: We thank Hydro for permission to publish this paper. Thanks also go to Tom Dreyer, Roger Walker, Alf Ryseth, John Gjelberg and Ian Sharp for use of their sedimentological interpretation of some of the cores. Thanks also to Olav Lauvrak for discussion about the temperature and burial history and Johannes Rykkje for help with SEM analyses. Thanks also to Hydros' Norwegian Sea exploration group at Kjørbo for help and comments. Thanks to Marianne Skibeli (ENI), Morten Smelror (NGU) and an anonymous referee for useful comments and corrections, and to Peter Padget for help with language vetting.

References

Ashely, G.A. 1990: Classification of large scale subaqueous bedforms: a new look at an old problem. *Journal of Sedimentary Petroleum 60*, 160-172.

Barclay, S.A. & Worden, R.H. 2000: Geochemical modeling of diagenetic reactions in a sub-arkosic sandstone. *Clay Minerals 35*, 57-67.

Bloch, S., Lander, R.H. & Bonell, L. 2002: Anomalously high porosity and permeability in deeply buried sandstone reservoirs: Origin and predictability. *American Association of Petroleum Geologists*, *Bulletin 86*, 301-328.

Bouma, A.H., 1962: *Sedimentology of some flysch deposits: a graphic approach to facies interpretation.* Elsevier, Amsterdam, 168p.

Brekke, H., 2000: The tectonic evolution of the Norwegian Sea Continental margin with emphasis on the Vøring and Møre Basins. In Nøttvedt, A. et al. (Eds.), *Dynamics of the Norwegian Margin.* Geological Society of London, Special Publication 167, 327-378.

Dalland, A., Worsely, D. & Ofstad, K. 1988: A lithostratigraphic scheme for the Mesozoic and Cenozoic offshore mid- and northern Norway. *Norwegian Petroleum Directorate, Bulletin 4*. 65 pp.

Doré, A.G. & Lundin, E.R. 1996: Cenozoic compressional structures on the NE Atlantic margin: nature, origin and potential significance for hydrocarbon exploration. *Petroleum Geosciences 2*, 299-311.

Ehrenberg, S.N., 1993: Preservation of anomalously high porosity in deeply buried sandstones by grain-coating chlorite: examples from the Norwegian continental shelf: *American Association of Petroleum Geologists, Bulletin 77*, 1260-1286.

Fjeldskaar, W., Johansen, H., Dodd, T.A. & Thompson, M. 2003: Temperature and maturity effects of magmatic underplating in the Gjallar Ridge, Norwegian Sea. In Düppenbecker, S., & Marzi, R. (Eds.), *Multidimensional basin modeling.* American Association of Petroleum Geologists/Datapages Discovery Series 7, 71-85.

Fonneland, H.C., Lien, T., Martinsen, O.J., Pedersen, R.B. & Kosler, J. 2004: Detrital zircon ages: a key to understanding the deposition of deep marine sandstones in the Norwegian Sea. *Sedimentary Geology 164*, 147-159.

Færseth, R. & Lien, T. 2002: Cretaceous evolution in the Norwegian Sea – a period characterized by tectonic quiescence. *Marine and Petroleum Geology 19*, 1005-1027.

Hiscott, R.N. 1979: Clastic sills and dykes associated with deep-water sandstone, Tourelle Formation, Ordovician, Quebec. *Journal of Sedimentary Petroleum 49*, 1-10.

Hjelstuen, B.O., Eldholm, O. & Skogseid, J. 1999: Cenozoic evolution of the northern Vøring margin. *Geological Society of America, Bulletin 111*, 1792-1807.

Lowe, D.R. 1975: Water escape structures in coarse-grained sediments. *Sedimentology 22*, 157-204.

Lowe, D. R. 1982: Sediment gravity flows II: Depositional models with special reference to the deposits of high-density turbidity currents. *Journal of Sedimentary Petrology 52*, 279-297.

Martinsen, O.J., Lien, T. & Jackson, C. 2005: Cretaceous and Palaeogene turbidite systems in the North Sea and Norwegian Sea basins: source, staging area and basin physiography controls on reservoir development. *In* Dorè, A.G. & Vining, B.A. (Eds.), *Petroleum Geology: North-West Europe and Global Perspectives – Proceedings of the 6th Petroleum Geology Conference*, Geological Society, London, 1147-1164. .

Mogensen, T.E., Nyby, R., Karpuz, R. & Haremo, P. 2000: Late Cretaceous and Tertiary structural evolution of the northeastern part of the Vøring Basin, Norwegian Sea. *In* Nøttvedt, A. et al. (Eds.), *Dynamics of the Norwegian Margin*. Geological Society, London, Special Publication 167, 379-396.

Middleton, G.V. & Hampton, M.A. 1976: Subaqueous sediment gravity flows. *In* Stanley, D.J. and Swift, D.J.P. (Eds.), *Marine Sediment Transport and Environmental Management*: Wiley-Intersci. Publication, New York, 197-218.

Ramm, M. 2000: Reservoir quality and its relationship to facies and provenance in Middle to Upper Jurassic sequences, northeastern North Sea. *Clay Minerals 35*, 77-94.

Riis, F. 1996: Quantification of Cenozoic vertical movements of Scandinavia by correlation of morphological surfaces with offshore data. *Global and Planetary Change 12*, 331-357.

Roberts, A.M., Lundin, E.R. & Kusznir, N.J. 1997: Subsidence of the Vøring Basin and the influence of the Atlantic continental margin. *Journal of the Geological Society of London 154*, 551-557.

Shanmugam, G., Lehtonen, L. R., Straume, T., Syvertsen, S. E., Hodgkinson, R. J. & Skibeli, M. 1994: Slump and Debris-Flows Dominated Upper Slope Facies in the Cretaceous of the Norwegian and Northern North Seas (61°-67°N): Implications for Sand Distribution. *American Association of Petroleum Geologists, Bulletin 78*, 910-937.

Skogseid, J. & Eldholm, O. 1989: Vøring Continental Margin: Seismic interpretation, stratigraphy and vertical movements. *In* Eldholm, O., Thiede, J. and Taylor,E. (eds.), *Proceedings of the Ocean Drilling Program, Scientific Results 104*, College Station, Texas, 993-1030.

Stow, D.A.V. & Johansson, M. 2000: Deep-water massive sands: nature, origin and hydrocarbon implications. *Marine and Petroleum Geology 17*, 145-174.

Vågnes, E., Gabrielsen, R.H. & Haremo, P. 1998: Late Cretaceous-Cenozoic intraplate deformation at the Norwegian continental shelf: timing, magnitude and regional implications: *Tectonophysics 300*, 29-46.

Walker, R.G. & Martinsen, O.J. 1999: Deep water facies and depositional environments, Cretaceous, mid-Norway: Conference Abstract: American Association of Petroleum Geologists/Society for Sedimentary Geology, Annual meeting 1999, Denver, USA.

Wilson, M.D. 1992: Inherited grain-rimming clays in sandstones from eolian and shelf environments: their origin and control on reservoir properties. *SEPM Special Publication 47*, 209-225.

Zeyen, H & Fernandez, M. 1994: Integrated lithospheric modeling combining thermal, gravity and local isostasy analyses: Application to the NE Spanish Geotransect. *Journal of Geophysical Research 102*, 18089-18102.